Development of sensing concrete: principles, properties and its applications

Siqi Ding [1], Sufen Dong [2], Ashraf Ashour [3], Baoguo Han [4, *]

[1] *Department of Civil and Environmental Engineering, The Hong Kong Polytechnic University, Hung Hom, Kowloon, Hong Kong*
[2] *School of Material Science and Engineering, Dalian University of Technology, Dalian, 116024 China*
[3] *Faculty of Engineering & Informatics, University of Bradford, Bradford, BD7 1DP, UK*
[4] *School of Civil Engineering, Dalian University of Technology, Dalian 116024, China*
* Corresponding author: hithanbaoguo@163.com, hanbaoguo@dlut.edu.cn

Synopsis:

Sensing concrete has the capability to sense its condition and environmental changes, including stress (or force), strain (or deformation), crack, damage, temperature and humidity through incorporating functional fillers. Sensing concrete has recently attracted major research interests, aiming to produce smart infrastructures with elegantly integrated health monitoring abilities. In addition to having highly improved mechanical properties, sensing concrete has multifunctional properties, such as improved ductility, durability, resistance to impact, and most importantly self-health monitoring due to its electrical conductivity capability, allowing damage detection without the need of an external grid of sensors. This tutorial will provide an overview of sensing concrete, with attentions to its principles, properties, and applications. It concludes with an outline of some future opportunities and challenges in the application of sensing concrete in construction industry.

Key words: Concrete; Sensing; Electrically conductive; Fillers; Pressure; Temperature; Humidity; Seebeck effect

List of Abbreviations

CB	Carbon black
CF	Carbon fiber
CNF	Carbon nanofiber
CNT	Carbon nanotube
DOS	Density of electronic states
FA	Fly ash
FBG	Fiber Bragg grating
GP	Graphite powder
MLG	Multi-layer graphene
NCB	Nano carbon black
NP	Nickel particle
PVAF	Polyvinyl alcohol fiber
RH	Relative humidity
SCC	Self-consolidating concrete
SDS	Sodium n-dodecyl sulfate
SF	Steel fiber

SHM	Structural health monitoring
SS	Steel slag
SSW	Super-fine stainless wire
TEP	Thermoelectric power

Contents

1. Introduction

Concrete, the most commonly used structural materials for construction of infrastructures from buildings to highways, dams, tunnels, bridges, high-rise towers and sewage systems, has been recognized for more than 200 years since the Roman Empire[1,2]. Produced by mixing water, aggregates and cement and allowing hardening, concrete is a durable, affordable, aesthetic and readily available composite material. However, physical effects including surface abrasion/erosion, cracking, aging, temperature variation and crystallization of salts in pores, penetration of water and fire or frost actions, associated with deleterious chemical effects such as alkali-aggregate reaction, carbonation, sulfate attack and corrosion of reinforcing steels, would cause deterioration of concrete[2]. The absence of advanced design and condition assessment tools and timely maintenance also plays a considerable role in the failure of concrete structures[3]. Therefore, surveillance, evaluation and assessment of the "health" of concrete structures at early stage to alleviate deterioration or avoid sudden accidents are of great importance to the extension of the service life and the security of lives and property. Inspired by the strategy implemented in human system, the process of monitoring changes that occur within concrete structures and providing real-time information of structural conditions for safety assessment and afterwards maintenance planning is known as structural health monitoring (SHM)[4–6]. To achieve this, an entire SHM system should include a sensory system, a data acquisition, transmission and management system, and an evaluation system. The fundamental part is to establish a stable and reliable sensing system, like "nervous subsystem", using appropriate sensing techniques. Up to now, for the purpose of diagnostics and evaluation of structural conditions,

a great number of sensing techniques have been developed and implemented with specific functions and mechanisms. For example, to evaluate the global behaviors of concrete structures such as change of frequency, modal assurance criterion, modal stiffness, modal flexibility, modal strain energy, frequency response function, model shapes and curvature, accelerometers, velocimeters and displacement transducers can be used directly via dynamic measurements[7–9]. To inspect damage in concrete structures, it can be realized with the help of techniques involving strain measurement such as strain gauges[10] or vision-based measurement such as video cameras[11]. To measure temperature and humidity inside concrete structures, the use of optical fiber sensors such as Fiber Bragg Grating (FBG) sensor has been very common[12]. Major achievements in the field of sensing techniques for SHM have been extensively reported by few literature reviews[6,13].

Although the development of SHM sensing techniques is relatively mature and many types of sensors have been successfully implemented on a tremendous of researches and for real SHM applications, the obvious drawbacks of high cost, time-consuming and labor-intensive installation and maintenance, unsatisfied performance in extreme environment and incompatibility with concrete structures limit their scalable implementation and deployment on civil infrastructures[3,14]. In light of the performance and complexity level, SHM sensing techniques can be classified into five levels from the simple one that detects the presence (Level I), location (Level II) and severity (Level III) of damage to the most complex Level V that enables the diagnosis and prognosis of damage by structure itself, and even self-healing function[15]. The existing SHM sensing technologies are still struggling at the primary levels, from Level I to Level III. For monitoring the change in structural health conditions, expensive, large and heterogeneous sensors or transducers have to be installed externally or internally in large quantities for the structures. Hence, there is a constant drive for development of advanced and high-level SHM sensing technologies.

With the rapid growth in modern science and engineering, it is unsurprising to imagine that if a concrete structure is so “smart/intelligent” or has its own sensing functionality so that it can assess the health conditions without integration of any extrinsic sensing elements. As an emerging sensing technology, sensing concrete with the capability to sense its condition and environmental changes has attracted significant interests and been envisioned to become the future of SHM. Sensing concrete, also known as intrinsic self-sensing, self-monitoring or self-diagnosing concrete, is fabricated through incorporating some functional fillers such as carbon fiber (CF)[16], carbon nanotube (CNT)[17], graphene[18] and nickel powder[19] into conventional concrete. The functional fillers with intrinsic sensing properties

usually are electrically conductive in nature. Well distributed functional fillers at a critical concentration will form an extensive conductive network inside concrete composite, making the composite conductive. Changes in the composite caused by external forces or environmental actions disturb the conductive network, leading to changes in the composite's electrical properties (usually electrical resistance). With this principle, stress (or force), strain (or deformation), crack, damage, temperature and humidity under static and dynamic conditions can be detected. Figure 1 presents the sensing concrete principle where conductive network constituted by functional fillers acts as "nervous system" to transduce signals stimulated internally and externally to computing center, i.e. "brain", mimicking human behavior. Compared with other smarter sensors used in SHM, sensing concrete has inherent hostile compatibility and identical lifespan due to its cement-based property when embedded inside concrete structures. In addition, with the functional filler reinforcement, sensing concrete exhibits remarkably enhanced mechanical properties and durability over the conventional concrete. The versatile, tunable and easy-to-scale features of fabrication process enables a great potential for mediating sensing concrete with a controlled composition, dimension, configuration and function to fulfill various engineering applications. Therefore, this smart material can be employed to produce intelligent infrastructure integrated with sensing and health monitoring abilities, thus improving serviceability, safety, reliability and durability of the infrastructures[3,20].

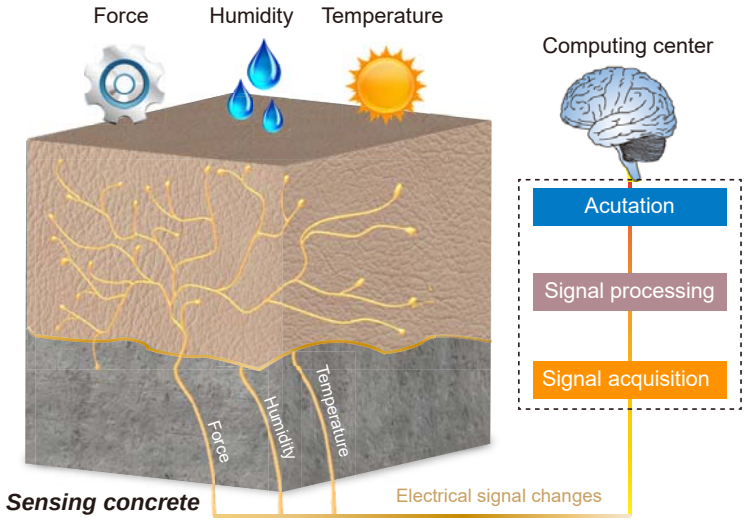

Figure 1 Sensing concrete mimicking human behavior: conductive network constituted by functional fillers acts as "nervous system" to transduce signals stimulated internally and externally to computing center, i.e. "brain".

Sensing concrete, a branch of smart concrete, refers to concrete materials and structures possessing properties to

sense various physical and chemical parameters related to structural integrity, durability and reliability in a generalized sense. On the basis of whether one or multiple sensing elements being integrated, the sensing concrete can be classified into non-intrinsic self-sensing concrete and intrinsic self-sensing concrete. For the non-intrinsic self-sensing concrete, as the name implies, external sensors or actuators such as strain gauges[21], optical fiber sensors[22], piezoelectric ceramics[23], electrochemical sensors[24], shape memory alloys[25] and conductive polymer composites[26] are embedded, attached or interfaced to enable concrete structures the sensing functions for structural health monitoring. In spite of generally using concrete materials as supporting structures, the function and performance of non-intrinsic self-sensing concrete is heavily determined by the integrated sensing elements, thus causing difficulties in mass production, high cost, signal acquisition and maintenance, etc[14]. For the intrinsic self-sensing concrete, it is, in essence, an electrically conductive concrete, fabricated by incorporating functional materials (usually conductive materials) into conventional concrete to render the ability of sensing strain, stress, crack, damage, temperature and humidity in itself while maintaining or even enhancing mechanical properties[20]. In a narrow sense, sensing concrete refers in particular to intrinsic self-sensing concrete. Note that the concept of sensing concrete mentioned in this tutorial refers to intrinsic self-sensing concrete unless otherwise stated. Since firstly discovered in 1992[16], sensing concrete has been witnessed significant progress and many innovative achievements have been gained in both its development and application over the past two decades. However, this SHM sensing technology is in its infancy, just like e-skin. Efforts on the development of sensing concrete are exciting technology and never-ending. In this tutorial, a brief definition and classification of sensing concrete are provided first, followed by its sensing principles and main properties including pressure-sensitive properties, temperature-sensitive properties, humidity-sensitive properties and Seebeck effect, specifically of intrinsic self-sensing concrete. Several applications for SHM of concrete structures and traffic detection are highlighted. Finally, this tutorial is summarized and future challenges for continued development and deployment of sensing concrete are also discussed.

2. Composition of sensing concrete

As a type of smart/functional composites, sensing concrete is generally comprised of two major phases: matrix materials and functional fillers. The matrix materials that serve as a binder as well as provide structural functions are cement-based composites including cement paste (only Portland cement)[27], cement mortar (Portland cement and fine aggregates)[28] and concrete (Portland cement, fine and coarse aggregates)[29,30]. Apart from Portland cement-based

composites, sulphoaluminate cement[31], geopolymer cement[32] and asphalt concrete[33] etc. have also been reported for using as matrix materials of sensing concrete. The mechanical behaviors (e.g., ultimate stress and strain, Young's modulus, and Poisson ratio) and sensing performance (e.g., sensitivity, repeatability, compatibility, and durability) of sensing concrete are highly dependent on the type and mix proportion of matrix materials. The functional fillers play an essential role in providing sensing ability as well as enhanced structural performance. The functional fillers varying from macroscale to nanoscale, fibrous to particle, single to hybrid and carbonaceous to metallic should be electrically conductive and chemically stable. Recent developments in nanomaterials have stimulated the use of functional fillers at the nanoscale[34–36]. Particularly promising functional fillers are nanocarbons including CNTs, carbon nanofibers (CNFs), nano carbon blacks (NCBs) and Multi-layer graphene (MLG) due to their excellent mechanical, thermal and electrical properties[37,38]. Table 1 summarizes the typically functional fillers used for sensing concrete.

Table 1 Categories of functional fillers in different classification criteria for sensing concrete

Classification			**Typical functional filler**
Criteria	Categories		
Material component	Carbonaceous		CF, CNF, CNT, CB, Graphite powder (GP), Graphene, Electrostatic self-assembled CNT/NCB, Electrostatic self-assembled CNT/TiO_2
	Metal or metal oxide		Super-fine stainless wire(SSW), Steel fiber(SF), Nickel particle(NP), Bi_2Te_3, Nano TiO_2, Fe_2O_3, ZnO, MnO_2 and Bi_2O_3
Filler shape	Flaky(2-D)		Graphene, MLG
	Fibrous(1-D)		CF, CNF, CNT, SF, SSW
	Particle(0-D)		CB, Steel slag (SS), NP, GP, Bi_2Te_3
Filler scale	Macroscale		SF, SS, SSW
	Microscale		CF, NP, Graphite
	Nanoscale		CNF, CNT, Graphene, Nano TiO_2, Fe_2O_3, ZnO, MnO_2 and Bi_2O_3
Conductive capability	Electrically conductive		CF, SF, CNF, CNT, CB, NP, SSW
	Semiconductive		Bi_2Te_3, Nano TiO_2, Fe_2O_3, ZnO, MnO_2 and Bi_2O_3, SS, Fly ash(FA),
	Nonconducting		Polyvinyl alcohol fiber (PVAF)
Application style	Single		CF, CNT, CB, SS, NP
	Hybrid	Fibers	CF and CNT, Copper coated CF and SF, PVAF and SF, PVAF and CF
		Fiber and particle	CF and CB, CF and GP, SF and GP, CNT and CB, Iron containing conductive aggregate and CF, PVAF and CB, CNT coated aggregate, Electrostatic self-assembled CNT/NCB, Electrostatic self-assembled CNT/TiO_2
		Particles	CB and NP, FA and SS
Surface state	Regular		CF, CNT
	Modified		Ozone-treated CF, CF treated by nitric acid or salt, Carbon coated nylon fiber, Copper coated CF, Hydroxyl CNT, CNT coated aggregate

3. Principles of sensing concrete

3.1 Electrically conductive mechanisms

At the microscopic level, concrete matrix after hydration is a solid-liquid-gas porous system[39]. On one hand, the water filling these voids or pores can dissolve ionic species (positive ions mainly including Ca^{2+}, Mg^{2+}, Al^{3+}, Fe^{2+}, K^{+} and Na^{+}; negative ions mainly including OH^{-} and SO_4^{2-}) from the solid phases, resulting in ionic conduction through the interconnected capillary pores. Since the ionic conduction is associated with the motion of ions in pore solution, ionic conductivity varies in a particularly wide range when cement contains a substantial amount of free water. On the other hand, electronic conduction through the gel, gel-water and untreated cement particles can contribute to the electrical conduction of concrete materials[40]. The two conduction paths can be visualized as the main conduction mechanism of conventional concrete. In dry conditions, concrete materials are quasi-insulators, generally having high DC electrical resistivity (10^6-10^9 Ω·cm) at room temperature[41]. The addition of functional fillers can decrease the electrical resistivity of sensing concrete to nearly 1 Ω·cm[42]. Similar to conductive polymer composites, the electrical conductivity of sensing concrete as a function of functional filler concentration is governed by percolation process[43]. The overall electrical conductivity of sensing experiences a rapid increase when the filler concentration reaches a critical filler concentration, i.e. percolation threshold, ϕ_c, which divides the conductive characteristic curve of electrical conductivity δ versus filler concentration ϕ into three zones: insulation zone A ($\phi < \phi_c$), percolation zone B ($\phi = \phi_c$) and conduction zone C ($\phi > \phi_c$), following a power law[44]:

$$\delta = \delta_f \left(\frac{\phi - \phi_c}{1 - \phi_c}\right)^{\gamma} \tag{1}$$

where δ_f is the conductivity of the filler, γ is the universal critical exponent. The percolation behavior strongly depends on the filler structure since it determines the neighbor closest-distance distribution function[45]. For example, the distance between spherical fillers d_s can be calculated by[46]:

$$d_s = \frac{a}{2}\left(\frac{4\pi}{3\phi}\right)^{\frac{1}{3}} \tag{2}$$

where a is the filler diameter. While the distance between fibrous fillers d_f can be calculated by[47]:

$$d_f = \frac{a}{2}\left(\frac{\pi l}{\phi}\right)^{\frac{1}{3}} \tag{3}$$

where l is the fiber length. Generally, fibrous fillers, having a high aspect ratio (a / l), can modify the electrical conductivity of sensing concrete at a much lower concentration level compared with spherical fillers.

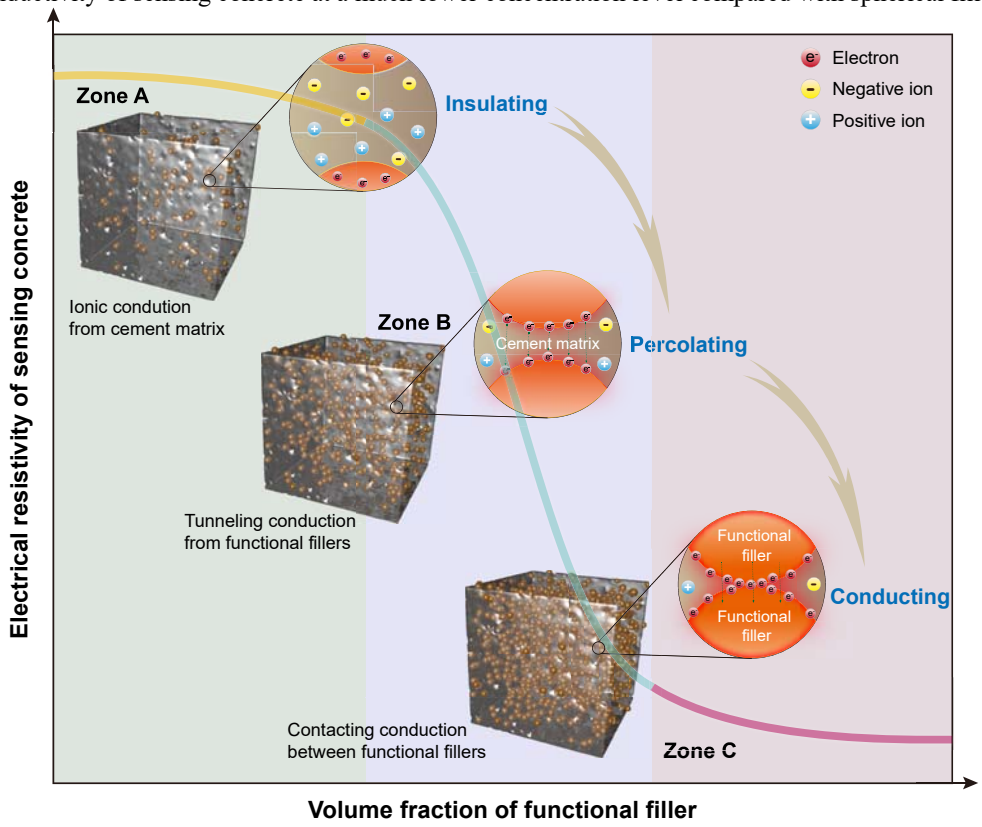

Figure 2 Electrically conductive mechanisms of sensing concrete during percolation process

The three zones exhibit different conduction mechanisms: ionic conduction for Zone A, tunneling conduction and/or field emission conduction for Zone B, and contacting conduction for Zone C, as shown in Figure 2. Note that the tunneling conduction is strongly related to the distance between two adjacent functional fillers, the local tunneling resistance R as a function of the inter-particle distance d can be described by[48]:

$$R = \frac{d\hbar^2}{Ae^2(2m\sqrt{\lambda})} e^{\left[\left(\frac{4\pi d}{\hbar}\right)\left(2m\sqrt{\lambda}\right)\right]} \tag{4}$$

where m and e are the mass and electric charge of an electron, $\hbar$ is Plank's constant, λ is the potential barrier height, A is the contact area of two fillers. It should be noted that field emission-induced tunneling conduction would

contribute for some functional fillers with nano-scale tips such as spiky nickel powder[19] and CNTs[49].

3.2 Sensing mechanisms

The sensing behavior of sensing concrete is essentially derived from variations in its electrical properties due to internal or external actions, in particular electrical resistivity. However, the manner affecting the electrical conduction is different for sensing concrete working with mechanical deformation or without mechanical deformation as explained below.

(1) With mechanical deformation. As shown in Figure 3, several changes are expected when sensing concrete is subjected to external force, including: (a) change of intrinsic resistivity of functional fillers, which is attributed to stress-induced local bonding deformation; (b) change of bonding between functional fillers and matrix, i.e. change of contact resistivity between filler and matrix due to filler pull-out and push-in upon tension and compression; (c) change of contact between functional fillers. The external force induces rearrangement and orientation of functional fillers, leading to the formation and destruction of effective conductive paths; (d) change of tunneling resistance between functional fillers, which is attributed to the variation of the inter-particle properties; (e) change of capacitance. Fibrous and flaky fillers can be regarded as capacitance plates due to the ionic conduction of concrete matrix. The external force leads to variations in the capacitance plate distance and the relative dielectric constant, resulting in the variation in capacitance[50].

In fact, the above-mentioned factors may work together for contribution to sensing property of sensing concrete, but only one or several of them plays the dominant role at a certain zone of the conductive characteristic curve. In Zone A, the conductive path is hard to form, even though an external force is applied to the composite. The change of capacitance is the dominant factor. As a result, the sensing concrete possess no or poor sensing property. At the beginning of Zone B, the change of capacitance, the change of intrinsic resistance of fillers, and the change of bonding between filler and matrix are the dominant factors. Near the percolation threshold, the leading factors become the change of tunneling distance between fillers, the change of contact between fillers, the change of bonding between filler and matrix and the change of intrinsic resistance of fillers. At the end of Zone B, the change of contact between fillers, the change of tunneling distance between fillers, and the change of intrinsic resistance of fillers play leading roles. Therefore, the sensing concrete at zone B has good sensing property. In Zone C, the change of contact between fillers and the change of intrinsic resistance of fillers become the dominant factors. The overall conductive network

stabilizes and changes little with the external force. As a result, the sensing concrete presents more stable sensing property and lower sensing sensitivity.

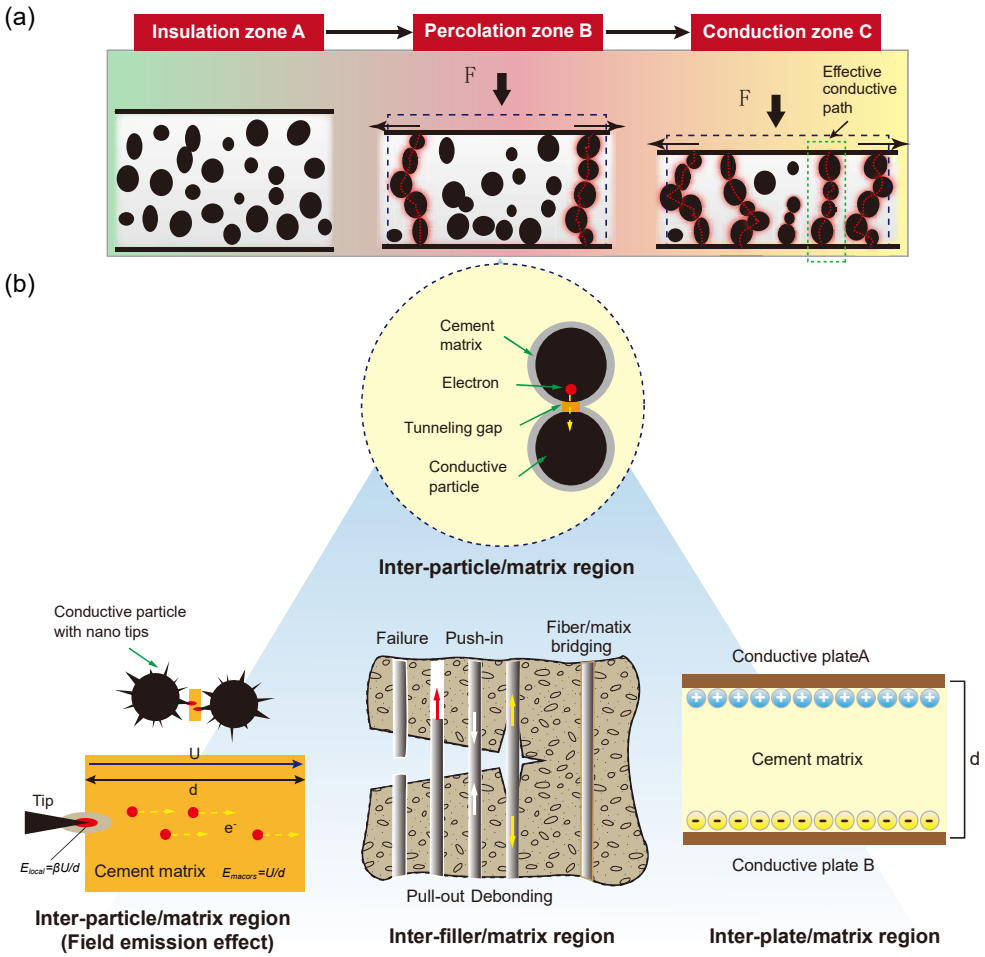

Figure 3 Sensing mechanism of sensing concrete under mechanical deformation. (a) Deformation-induced formation of effective conductive paths and (b) deformation-induced change of bonding, tunneling resistance and capacitance in the inter-filler region.

(2) Without mechanical deformation. Apart from mechanical deformation, factors including temperature and humidity can also lead to variation in electrical properties of sensing concrete. Temperature influences the electrical resistance of sensing concrete (i.e. temperature-sensitive property) by three means: (a) thermal deformation of concrete matrix, which has the similar mechanism with mechanical deformation mentioned above; (b) thermal activated charge

carriers (electrons, holes and ions)[51,52], which is in particular dominant at Zone A; (c) thermal fluctuation induced tunneling conduction, the tunneling current as a function of temperature T can be given as[53]:

$$J=\frac{c_1}{d^2}e^{\left(-c_0 d-\frac{Ea}{kT}\right)} \tag{7}$$

where $c_0=4\pi\sqrt{2m\lambda}/\hbar$, $c_1=\lambda BVe^2/\hbar\sin\pi BkT$, $B=2\pi A/\hbar\sqrt{2m\lambda}$, V is tunneling voltage, k is Boltzmann constant and E_a is activation energy. It can be seen that with an increase of temperature, an increase of tunneling gap and an increase of thermal fluctuation induced tunneling conduction have opposite effects on the change of electrical resistance. However, due to the negligible thermal deformation, the effect of thermal fluctuation induced tunneling conduction is dominant, i.e. the electrical resistance of sensing concrete decreases with increasing temperature[18].

In addition, if there is a temperature difference between two ends of sensing concrete, a voltage is generated due to the movement of charge carriers from high-temperature end to low-temperature end. This thermoelectric effect is known as Seebeck effect, which is the basis for thermocouples[54,55]. Based on this mechanism, it is feasible to use sensing concrete to monitor temperature in bulk concrete structures, which will be discussed in detail in Section 4.4.

Humidity influences the electrical resistance of sensing concrete (i.e. humidity-sensitive property) by three means: (a) change in structure of capillary pores, that is, water loss or invasion may lead to shrinkage or expansion of capillary pores[56], which can be negligible; (b) change in ionic conduction as water provides the transportation paths for ions, which is more significant for the Zone A[57]; (3) water absorption/desorption at the filler-matrix interface[28]. The presence of water would affect the contact resistance between filler and matrix, thus leading to variation in the bulk resistance of sensing concrete.

4. Properties of sensing concrete

Sensing concrete as new multifunctional material exhibits enhanced mechanical properties (such as strength and ductility) and durability (such as reduced permeability and shrinkage cracking) as well as additional functionalities as electrical, thermal, electromagnetic and sensing properties[34]. Based on the sensing principles of sensing concrete discussed above, this section will be devoted to the sensing properties of sensing concrete, mainly covering pressure-sensitive properties, temperature-sensitive properties, humidity-sensitive properties and Seebeck effect. Chemical-sensitive properties such as chloride-sensitive properties[58] and sulfate-sensitive properties[59] have not yet been fully

evaluated, therefore, not given in this tutorial. Other properties such as mechanical properties, durability and electromagnetic shielding of sensing concrete can be found in these reviews[34,35,38,60].

4.1 Pressure-sensitive property

The pressure-sensitive property or piezoresistivity, the most extensively explored sensing property of sensing concrete, refers to the ability to change the electrical resistivity of sensing concrete with external force or induced strain, with which the deformation and cracks of concrete structures can be detected. Several parameters including sensitivity, repeatability, hysteresis, signal to noise ratio, zero shifts, input/output range and linearity are used to characterize the pressure-sensitive property of sensing concrete[61], among which sensitivity and repeatability are the two most important factors. The sensitivity can be described as the maximum fractional change in electrical resistivity (i.e. $\max\left|\Delta\rho/\rho_0\right|$), force F sensitivity coefficient (i.e. $(\Delta\rho/\rho_0)/F$), stress σ sensitivity coefficient (i.e. $(\Delta\rho/\rho_0)/\sigma$) or strain ε sensitivity coefficient (i.e. gauge factor $(\Delta\rho/\rho_0)/\varepsilon$), where $\Delta\rho$ is change in electrical resistivity and ρ_0 is the initial electrical resistivity of sensing concrete. The repeatability can be characterized by the maximum difference in $\Delta\rho$ upon repeated measurement. The sensitivity and repeatability of sensing concrete evaluated by different loading conditions may be different, namely, sensing concrete features different pressure-sensitive characteristics when subjected to different loading conditions.

Figure 4 shows typical sensing behaviors of sensing concrete under monotonic loading, including compression, impact, tension and bending: (1) under monotonically uniaxial compression, fractional change in electrical resistivity $\Delta\rho/\rho_0$ experiences decrease, balance and abrupt increase states, which corresponds to compaction, fresh crack generation and crack extension, respectively. The moderate compaction leads to functional fillers getting close, thus enhancing the electrical conductivity of sensing concrete. With the increase of compression, fresh cracks are then generated inside the sensing concrete, causing competitive destruction and reconstruction of conductive paths. The fresh cracks are continuously extended, finally resulting in the breakage of conductive network, i.e. the occurrence of damage[62,63]. The pressure-sensitive characteristic under biaxial and isostatic compression is slightly different. The sensitivity in any stress direction during multiaxial compression is more sensitive than that during uniaxial compression due to the effect of multiaxial compression on postponing the emergence of fresh cracks, hindering them from opening[47,64]. (2) Under impact, the $\Delta\rho/\rho_0$ decreases abruptly and then goes back to zero after loading. The

$\Delta\rho/\rho_0$ depends on the amplitude of impact loads[65]. However, a high amplitude of impact or a sufficient number of impacts would make the $\Delta\rho/\rho_0$ unable to recover to zero due to the occurrence of damage inside the sensing concrete[66]. (3) Under monotonic tension, the $\Delta\rho/\rho_0$ is envisioned a linear increase with increasing tensile stress at first as the functional fillers trend to separate and microcracks open. After the ultimate tensile strain, the $\Delta\rho/\rho_0$ changes much faster due to the formation of damage. This means the sensing behavior of sensing concrete not only is a function of tensile strain but also is affected by the cracking behavior of the material when subjected to tension[67]. Therefore, the development and the mechanisms of the fracture process zone, and the estimation of propagating crack length can be in turn obtained from the electrical behavior of sensing concrete[68]. (4) Under bending, the coexistence of tension and compression sides of sensing concrete perform oppositely, consistent with the sensing behavior under tension and under compression alone with the measurement of surface resistance of the two sides. Meanwhile, the sensitivity in the tension side is usually much larger than its counterpart in the compression side under the same deflection of sensing concrete. This is attributed to the much higher compressive strength of sensing concrete than its tensile strength[69]. If the measurement of volume resistance or through-thickness resistance is used, the sensing behavior of sensing concrete becomes quite complicated, which strongly depends on the functional filler types and concentrations, notch depths and loading amplitudes[70–72].

The sensing behavior of sensing concrete under dynamic loading has also been extensively reported to evaluate its repeatability and sensitivity. Regardless of what kind of loading is applied, the $\Delta\rho/\rho_0$ always changes reversibly under cyclic loading with the amplitude below about 30% of ultimate strength of sensing concrete, i.e. sensing concrete in the state of elastic reversible deformation[18,62]. However, irreversible change of $\Delta\rho/\rho_0$ takes place in each cycle when the loading amplitude is over the elastic deformation range. In addition, there are some variations in the initial electrical resistivity of the sensing concrete after cyclic loadings. This is attributed to minor cracks and consequent reconstruction of conductive network inside the sensing concrete. With increasing loading cycles, the irreversibility increases due to the generation of permanent damage and deformations[63]. The sensing behavior of sensing concrete also exhibits a slight dependency on dynamic loading rate[73–75].

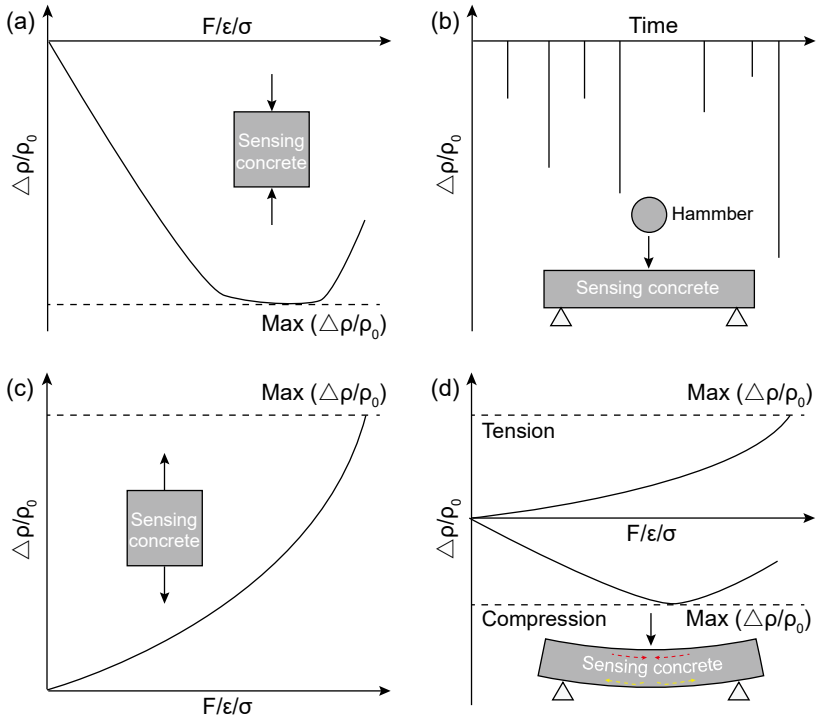

Figure 4 Typical sensing behavior of sensing concrete under monotonic loading including (a) compression, (b) impact, (c) tension and (d) bending.

From the above discussion, it is of great importance to fabricate sensing concrete with high sensitivity and good repeatability for real SHM application. The functional filler plays the most important role in determining the sensing property of sensing concrete as it dominates the formation and distribution of conductive network. Strategies to improve the sensitivity and repeatability of sensing concrete commonly focus on the optimization of the functional filler, as summarized in the following two aspects:

(1) **Optimization of functional filler itself**: The sensing property of sensing concrete can be optimized by tuning the concentration, geometrical shape and surface treatment of functional filler. To achieve a high sensitivity, the filler concentration near percolation threshold can be selected since there is an abrupt change of electrical conduction within the percolation zone. However, the sensing concrete with a high filler concentration above percolation threshold has better repeatability and stability due to the more stable conductive network inside[76]. The geometrical shape of functional filler has an effect on the distribution of conductive network and conduction mechanism of sensing concrete, as previously discussed in Section 3. In general, sensing concrete with conductive fibers such as CF, SF and CNT have better conductivity compared to sensing concrete with the same concentration of conductive powders such as

carbon black and slag powder due to their higher aspect ratio providing more conduction paths generation. Nano fibrous materials such as CNTs/CNFs, in particular, for their extremely high aspect ratio and specific surface area that can achieve electrical percolation at a low concentration are exceedingly desirable. Extensive research has shown that sensing concrete with CNTs/CNFs exhibits better mechanical properties and sensing performance than functional fillers at macroscale or microscale due to the nano-core effect[77]. However, a higher aspect ratio of conductive fiber means a higher probability of the agglomeration, which in turn effects the repeatability of sensing concrete. It has been confirmed that sensing concrete with conductive powders (carbon black) has more remarkable repeatability as they are easy to be strongly wrapped by cement matrix, thus less debonding and reorientation[78]. Therefore, recently, the combination of conductive powder and conductive fiber has been largely reported to improve both the sensitivity and repeatability of sensing concrete[75,79–81]. It is believed that the microscopic space between adjacent conductive fibers can be occupied by conductive powders, thereby resulting in enhanced electrical conductivity. Meanwhile, the resulting multiphasic and multiscale conductive network enables the sensing concrete more repeatable and stable[122–124]. Another approach to enhance the sensing behavior of sensing concrete relative to the geometrical shape of functional filler is to use nanoscale fillers or fillers with nano projections[73,74,82,83]. To date, the highest sensitivity of sensing concrete was reported by Han et al[83], achieving a gauge factor $(\Delta\rho/\rho_0)/\varepsilon$ of sensing concrete with nickel powder under compression as high as 1929.5, which is much higher than 560 of sensing concrete with CFs[84] and nearly 600 times of commercial strain gauge. The uniquely sharp nano-tips on the surface of the nickel powder can generate an enhanced local electrical field, thus decreasing the barrier height and width for interparticle electron tunneling conduction, i.e. field assisted tunneling conduction[85]. Table 2 lists the sensitivities of sensing concrete with typical functional fillers under different loadings.

Table 2 Sensitivity of typical sensing concrete under deformation

Filler type	**Sensitivity**					**References**
	$\max(\lvert\Delta\rho/\rho_0\rvert)$ (Under compression)	$(\Delta\rho/\rho_0)/\sigma$ (Under compression)	$(\Delta\rho/\rho_0)/\varepsilon$ (Under compression)	$(\Delta\rho/\rho_0)/\varepsilon$ (Under Tension)	$(\Delta\rho/\rho_0)/\varepsilon$ (Under Bending)	
CF	45%	-	560	90	-	Fu and Chung[63]
SS	50%	-	-	-	-	Han et al.[3]
CB	55%	-	50	-	-	Xiao[86]
NP	80%	0.16 MPa^{-1}	1500	8584	-	Han et al.[83]
SF	-	0.048 MPa^{-1}	720	4560	-	Chung et al.[84] Teomete et al.[87]

CNT	-	-	220	-	-	Materazzi et al.[73]
SSW	60%	0.324 MPa^{-1}	143	146.51	23.98	Dong et al.[88]
CNT/NCB	75%	2.32 MPa^{-1}	225.08	-	-	Han et al.[89]
MLG	35%	0.8 MPa^{-1}	156	-	-	Sun et al.[74]
CNT//TiO_2	84%	1.04 MPa^{-1}	217	-	-	Zhang et al.[17]

The surface treatment of conductive filler can also improve the repeatability of sensing concrete. Fu and Chung[63] found the sensitivity and repeatability of sensing concrete with Ozone-treated CFs were significantly improved in comparison to sensing concrete with untreated CFs owing to the enhanced bond strength between CF fibers and matrix. Similarly, sensing concrete with brass coated steel fiber also presented better repeatability and sensitivity as reported by Sun et al.[47]. The improvement due to surface treatment of conductive fillers is also contributed to the enhanced dispersion of fillers inside concrete matrix. Yu et al. found that sensing concrete with acid-treated CNTs showed stronger piezoresistive response and better repeatability than that with surfactant-wrapped CNTs as the surfactant could block the contacts among CNTs, thus impairing the piezoresistive response of the composite[90]. Han et al. employed a polycarboxylate superplasticizer to facilitate the dispersion of CNTs in cement paste. The surface carboxyl functionalization of CNTs can improve their wettability and reduce the tendency to agglomerate. As a result, sensing concrete with carboxyl CNTs was more stable and sensitive than that with plain CNTs[91].

(2) **Optimization of distribution of functional filler in matrix:** Under mechanical deformation, the conductive network constituted by functional fillers would be changed accordingly. It is exceedingly desirable to achieve uniform and stable distribution of functional filler in matrix since its high correlation with regards to the stability and repeatability of pressure-sensitive property of sensing concrete. The most effective method to enhance the distribution of functional filler in matrix, in particular nano-scale functional filler, is by using dispersion agents. The dispersion agents can be divided into three categories: surfactant, mineral admixture and micro-scale secondary filler. The mechanisms of surfactant are based on chemical and physical functionalization of nano-scale functional fillers to overcome the van der Waals attraction[92]. While enhanced dispersion using mineral admixture such as silica fume and micro-scale secondary filler such as graphite powder is based on gradation, adsorption and exclusion[93,94]. To change the local distribution of functional fillers in sensing concrete is one effective approach for controlling the sensing properties of sensing concrete. For example, Zhang at al. used secondary filler (i.e., TiO_2) to enhance the conducting network formed by CNTs in concrete matrix based on the excluded volume theory, thus improving the sensitivity of pressure-sensitive property[17]. For plain concrete, the electrical conductivity decreases as silica fume content increases,

which is attributed to its filling and pozzolanic effect that refines the microstructure and porosity of concrete, thus reducing the number and/or the mobility of charge carrying ions[95]. While for sensing concrete with conductive fibers such as CNTs, utilization of silica fume can improve the dispersion of CNTs due to its extremely fine particle size and enhance the interfacial interaction between CNTs and the hydration products due to its high pozzolanic activity[93]. Therefore, the electrical properties and pressure-sensitive property of sensing concrete are significantly improved[81,96–98]. While the addition of fly ash can improve the electrical conductivity of plain concrete due to its high content of Fe_2O_3. Similarly, good interaction between conductive fillers and fly ash cement matrix benefits the pressure-sensitive property of sensing concrete[89,99]. To achieve a desirable dispersion, dispersion agents combined with mechanical dispersion methods such as high shear mixing, ball milling and ultrasonication are often suggested. However, the dispersion agents and dispersion methods must be chosen carefully to preserve the integrity of functional filler, cement hydration and mechanical properties of concrete matrix. In the case of sensing concrete with aggregates, the interaction and separation of aggregates with functional fillers would induce higher electrical resistivity and poorer sensing performance than sensing concrete without aggregates[30]. A novel method to improve the distribution of functional fillers in sensing concrete with aggregates is to modify the cement matrix-aggregate interface or interfacial transition zones with functional filler-based thin films. The highly conductive thin films can be deposited directly on fine and coarse aggregates using airbrushing or spray coating. In this way, the functional fillers are uniformly dispersed throughout concrete along with the aggregates, thus establishing a stable conductive network[100].

Besides, water as a main raw material for fabrication of sensing concrete also plays a key role in adjusting the distribution of functional filler in matrix. A higher water/cement ratio helps the pre-dispersion of functional filler in water but has a negative impact on the dispersion of functional filler in matrix due to the re-agglomeration of the functional filler during mixing and molding process, resulting in weakened electrical conductivity. In addition, under cyclic loading, the shrinkage-recovery behavior of sensing concrete and conductive network is worsened when the water/cement ratio is high, indicating diminished repeatability of sensing concrete[101]. Therefore, a low water/cement ratio is preferable with regards to the improvement of the repeatability of sensing concrete. It is noted that water can also affect the sensitivity of sensing concrete. On one hand, the adsorption of water on conductive filler gives rise to the change in the intrinsic resistance of the filler. Especially, water attracted to the CNT tips makes the highly occupied molecular orbital unstable, thereby enhancing the field emission on the CNT tips. The sensitivities of sensing concrete

with CNTs first increase, then, decrease with the increase of water content in the composites[102]. However, the sensitivities of sensing concrete with CNTs/NCBs all increase with the increase of water content due to the decreased contact resistance between filler particles[28]. On the other hand, the electronic and electrolytic conduction characteristics of sensing concrete are strongly affected by the water/cement ratio. An increase in the water/cement ratio degrades the continuity of functional fillers in a cement matrix which in turn significantly increases the electrical resistivity of the sensing concrete. In addition, an increase in the water/cement ratio increases the influence of the electrolytic pore solution on the electrical resistivity of the composites and, thereby, leads to instability of the electrical resistivity[103]. The water/cement ratio would also affect the deformation capacity of sensing concrete and dispersion of conductive filler in sensing concrete. A higher water/cement ratio leads to a lower elastic modulus, which is beneficial for the improvement of sensitivity of sensing concrete[104].

4.2 Temperature-sensitive property

Sensing concrete is known to be similar in behavior to a semiconductor, which exhibits a negative temperature coefficient of electrical resistivity, i.e. electrical resistivity of sensing concrete decreases with increasing temperature. The temperature-resistivity behavior is not only useful for sensing concrete to serve as temperature sensors, it is relevant to the understanding of its electrical conduction mechanisms. The electrical conductivity δ_T of sensing concrete as a function of temperature T can be related to its conductivity δ_r at a reference temperature T_r, by the formula:

$$\delta_r = \frac{\delta_T}{\left[1+\alpha\left(T-T_r\right)\right]} \tag{8}$$

where α is a temperature coefficient for sensing concrete. This formula is only applicable for fully saturated concrete under a narrow range of temperatures, typically $\pm 5℃$ around the reference temperature. As the ionic conduction of cement matrix depends on both the concentration and mobility of ionic charges in the pore network, the activation energy approach for ion mobility governed by the Arrhenius equation is more frequently used to describe the temperature-resistivity behavior of sensing concrete, given by[105]:

$$\delta = \mathrm{C}_p e^{-\left[\frac{E_a}{C_g T}\right]} \tag{9}$$

where C_p is a pre-exponential constant, C_g is the gas constant (8.314 J/mol/K) and E_a is the activation energy for

the conduction process, which reflects the energy for the hopping of the charge carrier in the composite. As the activation energy quantifies the amount of thermal energy required for a reaction or transportation process to proceed, the calculated activation energy values can be interpreted as the amount of thermal energy needed in the bulk concrete to facilitate electrons jumping between conductive fillers through the concrete matrix. Lower activation energy values indicate improved percolation pathways for electron transport and reduced the potential needed for electron tunneling through the cement paste. Therefore, the sensitivity of sensing concrete can be described by the activation energy, as obtained from the negative slope of the Equation (9) plot of the logarithm of conductivity against the inverse of temperature. The sensitivity can be also described by temperature sensitivity coefficient (i.e. $(\Delta\rho/\rho_0)/T$. The temperature-sensitive property of sensing concrete has been found to be highly dependent on many factors, including water/cement ratio[40,106,107], functional filler concentration[18,108,109], filler type[105,109–111] and supplementary cementitious material[112].

Wen et al. firstly reported the temperature--sensitive property of sensing concrete with CFs[112]. Figure 5 shows the typical temperature-resistivity characteristic of sensing concrete with CFs during stepped heating and cooling. It can be observed that the electrical resistivity decreased as temperature increased from 0-45℃, and returned back in the cooling process. However, the resistivity was slightly increased after heating and cooling cycle, which is explained by the thermal degradation of the sensing concrete[112]. The Arrhenius plot gives the activation energy, 0.39±0.014 eV during heating and 0.412±0.017 eV during cooling, respectively. Compared to sensing concrete without CFs (0.035±0.003 eV for heating and 0.084±0.004 eV for cooling), the presence of CFs can significantly increase the activation energy due to the hopping conduction between cement matrix and CF. However, the CF volume fraction below the percolation threshold leads to the insignificant effect of direct electronic conduction through CF network. McCarter et al. studied the temperature-sensitive property of sensing concrete with 3 mm and 6 mm CFs at a volume fraction of 0.5 %, which is within the percolation zone[111]. The activation energies of sensing concrete with CFs (0.055 eV for 3 mm CFs and 0.035 eV for 6 mm CFs) were considerably lower than that of conventional concrete (0.20 eV), which is totally opposite with the result reported by Wen et al[112]. The difference is attributed to the high volume fraction of CFs exerting a significantly influence on conductive network inside the composite. Within the percolation zone, tunneling conduction and ohmic contacting conduction would dominate in sensing concrete with CFs, hence lowering the activation energy compared to the conventional concrete in which ionic conduction is dominated, i.e.

lower sensitivity of temperature-sensitive property. Sun et al. investigated the temperature-sensitive property of sensing concrete with different volume fraction of MLGs[18]. They found that when the volume fraction of MLGs was below the percolation threshold (2 vol. %), the temperature-sensitive property of sensing concrete was similar to that of the conventional concrete. With the increase of the volume fraction of MLGs, the sensitivity of the temperature-sensitive property appeared a decreasing trend. However, thermal conductivity of sensing concrete with MLGs increased as the is consistent with sensing concrete with different contents of CNT/NCBs[108] and CNT/CFs[107]. Kim et al. attributed the lower sensitivity to the difference in the thermal expansion coefficient between fillers and cement. The coefficient of thermal expansion of cement was ten times higher than that of CNT/CFs, thus the thermal expansion behavior of sensing concrete with CNT/CFs was dictated by the cement rather than CNT/CFs. Moreover, the addition of CNT/CFs extends and stabilizes the conductive paths of the sensing concrete and mitigates the effects of thermal expansion on the continuity of conductive path, hence resulting in lower sensitivity but better repeatability, indicating that thermal expansion plays an insignificant role in the temperature-sensitive property of sensing concrete. In fact, at low temperature, this deformation can be neglected due to extremely low thermal expansion coefficient of concrete matrix (10^{-6}/℃)[113]. However, as temperature increased up to 150℃ or above, structural breakage due to water loss from hydrated cement paste and internal collapse of sensing concrete occur, leading to an abrupt increase of electrical resistivity of sensing concrete. Egemen et al. reported a rapid electrical resistance increase from 351 Ω to 39000 Ω at 243℃ for sensing concrete with 1 vol. % brass coated steel fibers[87], and from 700 Ω to 2893 Ω at 150 ℃ for sensing concrete with 0.8 vol. % brass fibers[114], as shown in Figure 6. Therefore, the sensing concrete can be used as fire alarm sensor for fire protection.

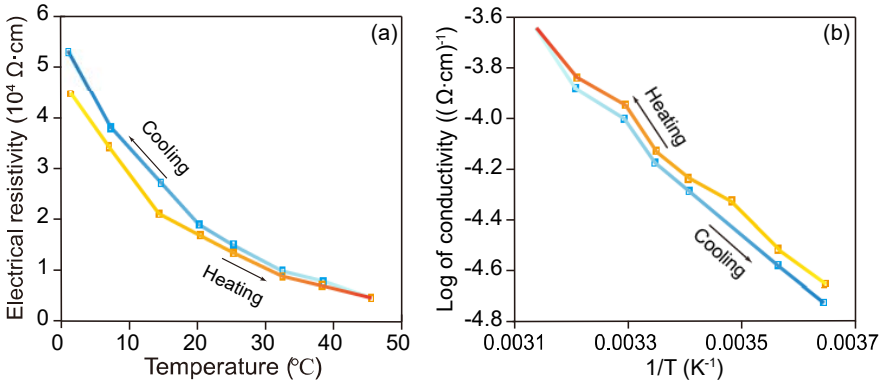

Figure 5 The temperature-sensitive property of sensing concrete with CFs. (a) Electrical resistivity as a function of temperature during heating and cooling, (b) Arrhenius plot of log electrical conductivity as a function of inverse absolute temperature during heating and cooling[112].

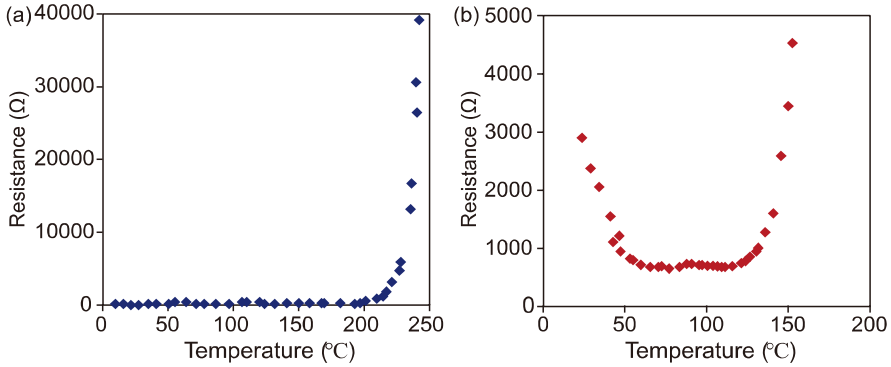

Figure 6 The temperature-sensitive property of sensing concrete (a) sensing concrete with 1 vol. % brass coated steel fibers[87], and (b) sensing concrete with 0.8 vol. % brass fibers[114].

Surface treatment of functional filler can also reduce the activation energy of sensing concrete. Chang et al. compared the temperature-sensitive property of sensing concrete with surfactant (sodium n-dodecyl sulfate, SDS) treated CFs and untreated CFs and found that surfactant treated CFs weakens the relationship between temperature and resistivity and improve the electrical conductivity by lowering the activation energy for electrons hopping from fiber to fiber, which can be interpreted as the result of improved dispersion and reduced distance between CFs[109]. Oppositely, due to the surface chemistry interaction between the negatively charged SDS and CFs, the activation energy of individual CF would be increased, resulting in stronger temperature-resistivity dependency. Therefore, as shown in Figure 7, adding a higher concentration of surfactant treated CFs (0.75 wt. %) yielded higher electrical resistivity of sensing concrete in comparison to that with 0.5 wt. % of surfactant treated CFs. However, the overall reduction of activation energy in the treated CFs cases implied the dominant role of the improved dispersion of CFs, which was further verified using self-consolidating concrete (SCC) instead of ordinary concrete in Chang's work[109]. Due to the low viscosity and high flowability of SCC concrete, CFs would be effectively dispersed using SSC mix procedure, viewing a more notable reduction of electrical resistivity and lowest activation energy for the SCC with 0.5 wt. % CF. The higher CF concentration (0.75 wt. %) in the SCC produced a slight increase in both electrical resistivity and activation energy due to reduced flowability.

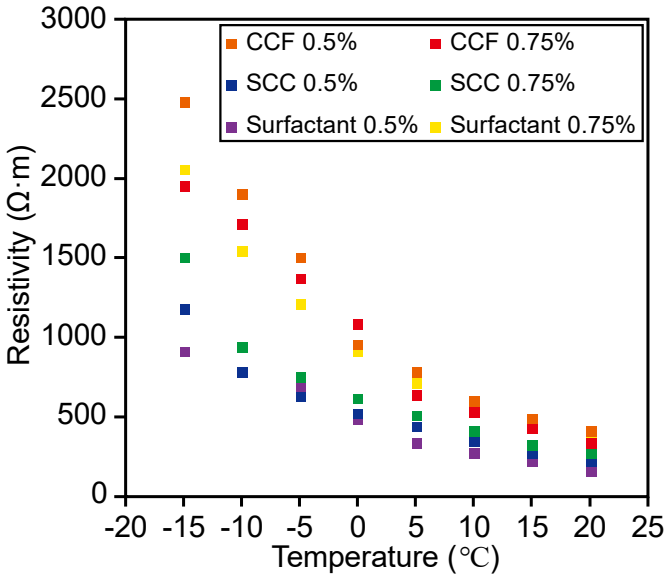

Figure 7 The temperature-sensitive property of sensing concrete with untreated and treated CFs[109].

4.3 Humidity-sensitive property

Monitoring the water movement inside concrete is of particular interest to civil engineers as water plays an important role in hydration as well as deterioration process in concrete. The humidity-sensitive property of sensing concrete based on electrical resistivity measurement provides a new perspective to measure internal humidity of concrete and environmental humidity surround its service condition. In general, water in concrete is presented in three states: as free water held by capillarity, as absorbed water held by surface forces and as bound water held chemically. The first two states of water, also called free water, are physically bound to concrete and can be lost or gained by being exposed to the environment or can be evaporable when oven drying at 105°C. The rest water chemically bounded with hydration products just evaporates at temperatures up to 500 °C. Therefore, the effect of moisture content (or internal humidity) on the electrical resistivity of sensing concrete is mostly attributed to the free water. Due to a change in the amount of free water, caused by variation in either internal humidity or environmental humidity, the electrical resistivity of sensing concrete would be changed, namely humidity-sensitive property of sensing concrete. Herein, it is necessary to distinguish that the term “humidity” refers to the presence of water in gaseous form present in the environment, while the term “moisture” refers to the water in liquid form that may be present in solid concrete matrix. The term “relative humidity”(RH) represents the ratio of the partial water vapor pressure (P_w) present in the

environment to the saturation water vapor pressure(P_s), i.e. $RH = \left(P_w / P_s\right) \times 100\%$ [115]. Since humidity is the frequently used expression in the field of measurement, it is adopted throughout this tutorial interchanged with moisture or water content.

The most common phenomenon for internal humidity-sensitive property of sensing concrete is that the electrical resistivity of sensing concrete sequentially increases with curing ages due to water loss for cement hydration[56,88,116]. As shown in Figure 8(a), the effect of humidity on the electrical resistivity of sensing concrete is pronounced with the decrease of functional filler content. The most considerable variation in the electrical resistivity is observed for sensing concrete without functional filler[88]. Chen et al. also observed that the internal humidity has an influence on the conductivity in the case of the sensing concrete containing low CF contents and this influence becomes less with increasing fiber content[116]. In addition, Reza et al. found that the electrical resistivity of sensing concrete with CFs was less sensitive to environmental humidity while the electrical resistivity of sensing concrete without CFs exhibited significant variation as shown in Figure 8(b)[117]. The more pronounced effect of humidity on conventional concrete than on the sensing concrete is attributed to their different conductive mechanisms. Sensing concrete is a composite system constituting n percolated phases of which the effective electrical conductivity σ_e can be described by a modified parallel law[118]:

$$\sigma_e = \sum_{i=1}^{n} \left(\sigma_i \phi_i \beta_i\right) \tag{10}$$

where σ_i , ϕ_i and β_i are the electrical conductivity, volume fraction and the connectivity factor of each constitutive component (i) including conductive filler phase, liquid phase, solid phase and gaseous phase. It is reported that liquid conductivity is usually in the range ($\sigma_{liq} \approx$ 1–20 S/m), conductivity of solid and gaseous phases are estimated as $\sigma_{sol} \approx 10^{-9}$ S/m and $\sigma_{gas} \approx 10^{-15}$ S/m, respectively[118]. Assuming that only the conductive filler phase and liquid phase contribute to the electrical conduction of sensing concrete, Equation 10 can be simplified to the following form:

$$\sigma_e = \sigma_{liq} \phi_{liq} \beta_{liq} + \sigma_f \phi_f \beta_f \tag{11}$$

where σ_{liq} , ϕ_{liq} and β_{liq} are the electrical conductivity, total liquid filled porosity and pore connectivity of the liquid phase, σ_f , ϕ_f and β_f are the electrical conductivity, volume fraction and filler connectivity of the conductive filler

phase. As electrical conduction of sensing concrete is dominated by electronic conduction due to the electronic nature of conductive filler phase, rather than ionic conduction dominated for conventional concrete, in which the electrical conduction occurs through its liquid phase ($\sigma_f >> \sigma_{liq}$). Furthermore, when conductive filler content is above percolation threshold at which the fillers touch each other to form a continuous electrically conductive path, indicating high values of ϕ_f and β_f. Therefore, the role of the liquid phase in conduction is diminished for sensing concrete, resulting in less sensitive humidity-sensitive property of sensing concrete than conventional concrete, which is particularly obvious at a higher filler content[88,116,117].

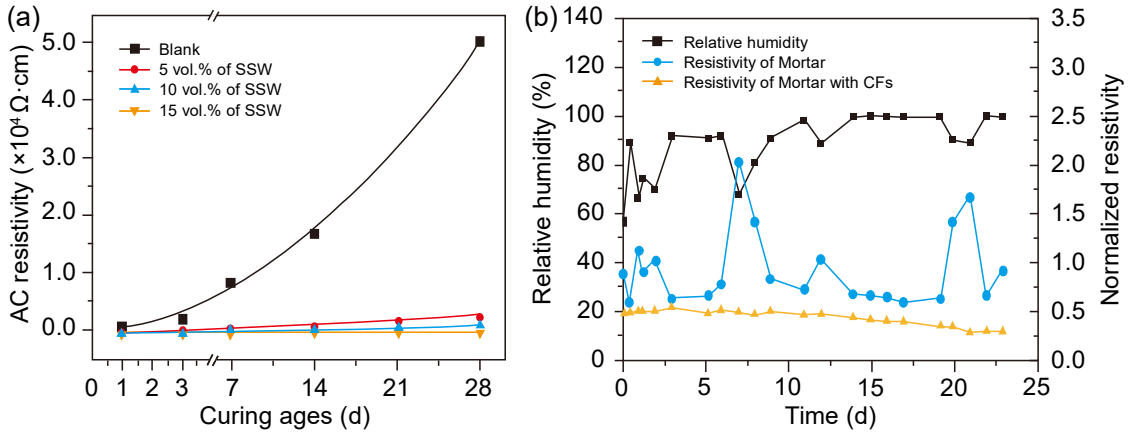

Figure 8 (a) Electrical resistivity of sensing concrete with short-cut super-fine stainless wire as a function of curing age[88] and (b) Change in electrical resistivity with relative humidity for sensing concrete with CFs and without CFs[117]

According to Equation 11, the humidity-sensitive property of sensing concrete is not only highly relevant to the conductive filler volume fraction, it also depends on the functional filler type. Different functional fillers have different intrinsic electrical conductivity, water adsorption property as well as filler connectivity. Sun et al reported that the electrical resistivity of sensing concrete with CFs under oven curing was more than two times higher than that under air curing[47]. Similar result was also reported by Cao et al that the electrical resistivity of sensing concrete with CFs was much lower in wet state than in dry state[57]. However, Han et al. reported that sensing concrete with CFs and CBs exhibited an opposite trend as shown in Figure 9, the electrical resistivity of sensing concrete with CFs and CBs was measured at different drying time and different soaking time using DC four-electrode method[119]. During drying and soaking, the electrical resistivity of sensing concrete with CFs and CBs gradually decreased and increased as a function

of time, respectively. In spite of sensing concrete with CFs only or with CFs and CBs, the humidity variation after soaking generally decrease the electrical resistivity due to enhanced ionic conduction[57]. However, changes in electrical resistivity of CFs and CBs due to water adsorption are different. For sensing concrete with CFs and CBs, the change in electrical resistivity is mainly caused by CBs due to their high water adsorption property. The water absorption on CBs can significantly increase the contact resistance between carbon black particles and decrease its electrons and holes conduction[119]. Zhang et al. studied the relationship between fractional change in electrical resistivity and time in a curing box with a RH of 95% for 20 min[28]. As shown in Figure 10, the electrical resistivity of all the conductive fillers increased with increasing time because of continuously adsorbing water increasing the contact resistance between fillers and matrix. In addition, humidity has the most significant effect on the electrical resistivity of CBs[28]. This verified that change in electrical resistivity of sensing concrete with CFs and CBs with humidity was mainly determined by CBs. Egemen et al found that there is an optimum humidity below which the water acting as electrolyte in the pores determined the change in electrical conductivity of sensing concrete, while above which water induced contact resistance between filler-filler and filler-matrix would play a dominant role. The evolution of electrical resistance of sensing concrete with steel fiber as a function of humidity therefore exhibited a first decrease and then increase[87,114].

However, the utilization of sensing concrete as humidity sensors is still a challenging issue due to a significant water desorption-absorption hysteresis of concrete materials. The water sorptivity coefficient k_s can be determined by:

$$\frac{Q}{A_w} = k_s\sqrt{t} \tag{12}$$

where Q is the amount of water absorbed, A_w is the cross-sectional area of the sensing concrete being in contact with water and t is the time. The water permeability k_f can be derived from Darcy's law:

$$k_f = \left(\frac{a_w \times l_c}{A_c \times t}\right)\ln\frac{h_i}{h_f} \tag{13}$$

where A_c is the cross-sectional area of the sensing concrete, a_w is the cross-sectional area of water input, l_c is the sensing concrete thickness, t is the time, h_i and h_f are the initial and final water heads. From the above two equations,

it can be obtained that the water sorptivity and water permeability are both functions of time, which leads to the hysteresis of humidity-sensitive property of sensing concrete. The addition of functional fillers can further decrease water sorptivity and water permeability of sensing concrete due to the modification of hydration products, reduction of porosity and autogenous shrinkage[120,121]. As shown in Figure 11, both sensing concrete with CNTs demonstrated lower amounts of absorbed water and lower sorptivity coefficient than conventional concrete[120]. In addition, water penetrated to a lower level in the sensing concrete with graphene than conventional concrete. The maximum distance between the initial water level and the infiltration level is as a function of graphene content, which decreased with the increasing content of graphene[121]. Therefore, a low hysteresis porous material such as siltstone can be used as the matrix material of sensing concrete to facilitate the measurement of internal and external humidity of concrete structure[118].

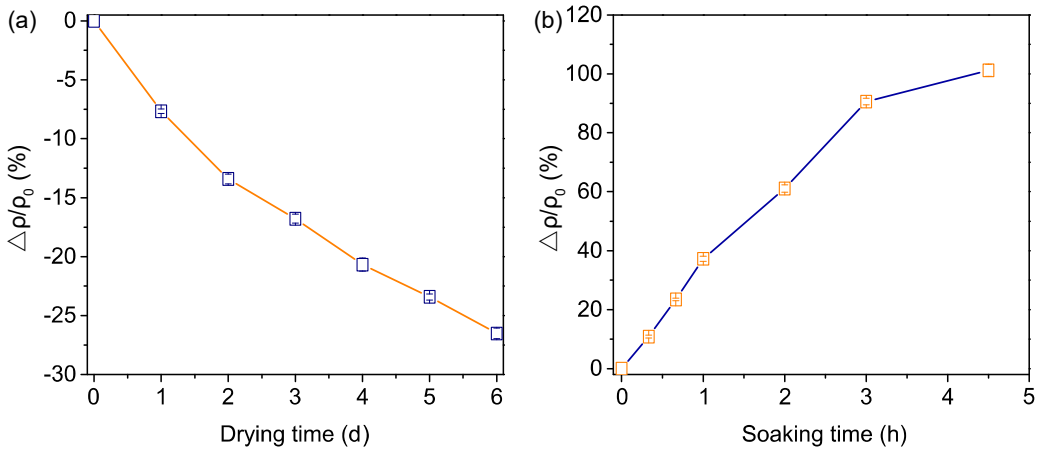

Figure 9 (a) Fractional change in electrical resistivity of sensing concrete with CFs and carbon black during soaking and (b) fractional change in electrical resistivity of sensing concrete with CFs and carbon black during drying[119]

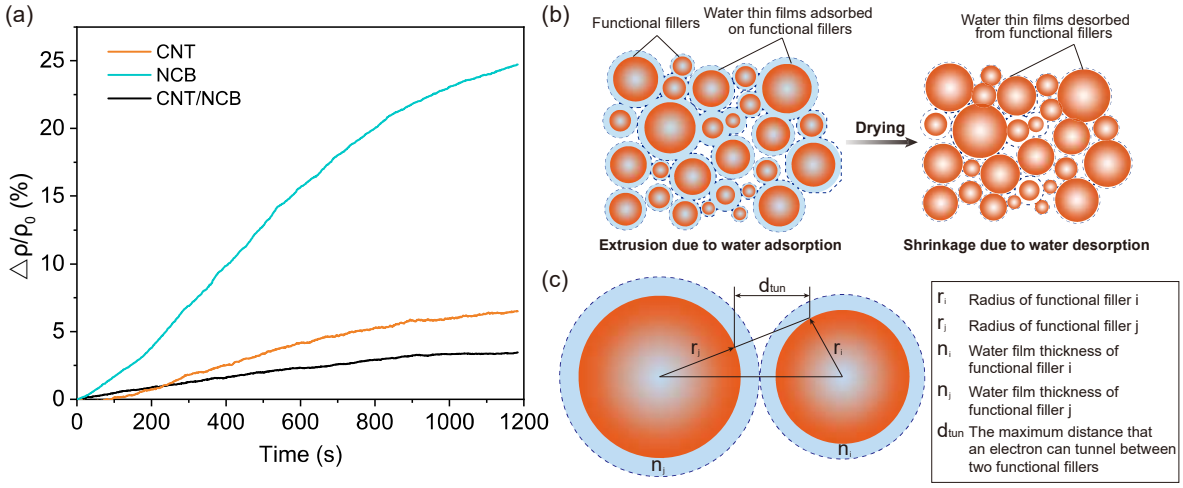

Figure 10 (a) Change in electrical resistivity of CNTs, NCB, and CNT/NCB composite filler in a curing box with a RH of 95% for 20 min[28], (b) Schematic of effect of humidity on the contact resistance of functional fillers and (c) charge transfer between two functional fillers covered by water films, which increase the energy barrier for electron tunneling.

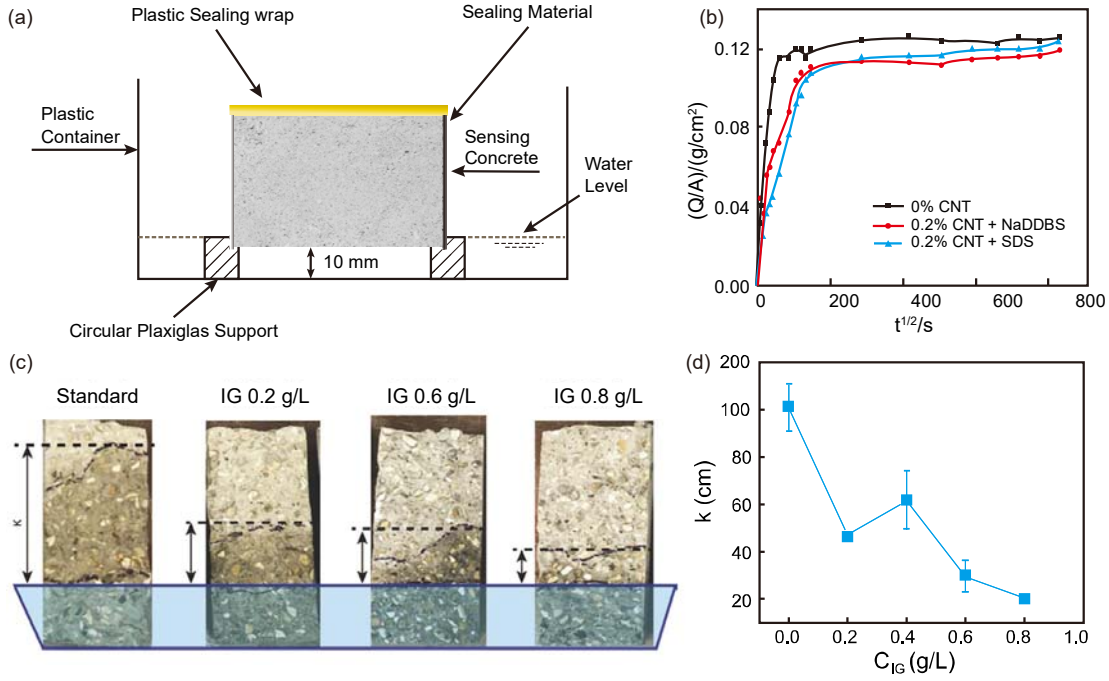

Figure 11 (a) Experimental setup for water sorptivity test, (b) relationships between water absorbing amounts and water absorbing time of sensing concrete with and without CNTs[120] (c) water permeability of sensing concrete with and without graphene after 7 d in water and (d) the maximum depth of water penetration in sensing concrete with and without graphene after 7 d in water[121].

4.4 Seebeck effect

Seebeck effect refers to the thermoelectric effect in which a voltage is generated by a temperature gradient due to the movement of charge carriers (electrons or holes) between hot end to cold end. The Seebeck effect can be described by the thermoelectric power (TEP) or Seebeck coefficient (S) as:

$$S = \frac{\Delta V}{\Delta T} \tag{14}$$

where ΔV is the electric potential difference generated by a temperature gradient ΔT. Figure 12 shows schematic illustration of the set-up for Seebeck coefficient measurement. If a majority of carriers are holes (positive charge), the Seebeck coefficient is positive, i.e. p-type behavior. If a majority of carriers are electrons (negative charge), the Seebeck coefficient is negative, i.e. n-type behavior[122,123]. With this principle, the thermoelectric material is popular to be used in temperature monitoring, energy harvesting and air conditioning[52,124,125]. However, conventional concretes have been observed as weakly n-type semiconductors with a low absolute Seebeck coefficient of 10^{-5}-10^{-4} V/℃[122], restricting their applications in the field of sensing and energy harvesting. To solve this problem, considerable attention has been paid to increase Seebeck effect of sensing concrete using various functional fillers, including carbon materials, metal material and metal oxides as discussed below.

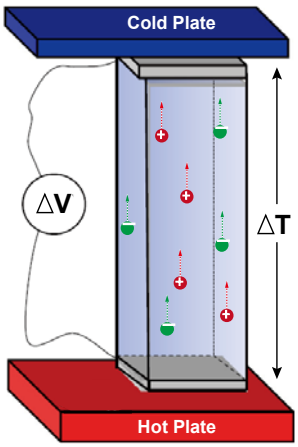

Figure 12 Schematic illustration of the set-up for Seebeck coefficient measurement.

(1) **Carbon material**: Carbon materials used to enhance the Seebeck effect of sensing concrete mainly include CF, graphite, expanded graphite and CNT. Sun et al. firstly improved the Seebeck effect of sensing concrete by adding

CFs. The presence of CFs provided a large excess of positive holes for hole conduction, thus increasing the Seebeck coefficient to 12 μV/℃[126]. Intercalating CF by bromine to form an intercalation compound between the graphite layers can further increase carrier concentration of CFs. The bromine as a hole metal can accept electrons from the CFs, resulting in a large increase in the hole conduction. The Seebeck coefficient of sensing concrete with bromine-intercalated CFs can be increased to 21.2 μV/℃[127], which is much higher than that with amorphous pristine CFs (0.89 μV/℃) and with crystalline pristine CFs (0.47 μV/℃)[110]. The addition of graphite into sensing concrete with CFs has also exhibited significant increase in the Seebeck effect as its highly anisotropic thermal conductivity and electrical conductivity can reduce the transition barrier of carries between CFs[125,128]. In contrast to CFs, CNTs have an extraordinary 1D tubular structure composed of graphite sheets and have significant influence on the thermoelectric effect by enhancing the hole conduction. The enhancement was not related to the improvement of the density of states near the Fermi energy of CNTs by reducing dimensions. The quantum confinement also increased electronic mobility of CNTs, leading to the increase of the Seebeck coefficient[129].

(2) Metal materials: Due to a large number of electrons carriers in metal materials, sensing concrete with metal materials is expected to have a high Seebeck coefficient. For example, sensing concrete with 1.0 wt.% of steel fibers can obtain a Seebeck coefficient of 68 μV/℃. This value was as high as that of commercial thermocouple materials. The steel fiber itself has a positive Seebeck coefficient so that the interface between steel fiber and cement paste is junction of electrically dissimilar materials, like a pn-junction, resulting in high Seebeck coefficient for sensing concrete with steel fibers[54].

(3) Metal oxide: However, the obtained Seebeck coefficients of the sensing concretes mentioned above are below 100 μV/℃. Due to the merits of wide energy gap, high temperature stability, tunable electronic and phone transport properties and well-established synthesis techniques, using metal oxides with high Seebeck coefficients as functional fillers is an effective approach to enhance the Seebeck effect of sensing concrete. In addition, the interface between metal oxides and cement paste would scatter hole carriers emerging from metal oxide intensively though energy-filtering effect and energy-selective carrier scattering. In addition, the increased surface density of the electronic state near the Fermi energy level of the nanostructured metal oxide further enhances the Seebeck coefficient[130]. As the system dimensionality decreases, it is possible to cause dramatic differences in the density of

electronic states (DOS), allowing new opportunities to enhance Seebeck coefficient. Figure 13 shows that nanostructured materials exhibit sharper DOS compared to higher dimensional structures, which is predicted to be the best for thermoelectric materials. Table 3 lists the Seebeck effect of sensing concrete with different functional fillers.

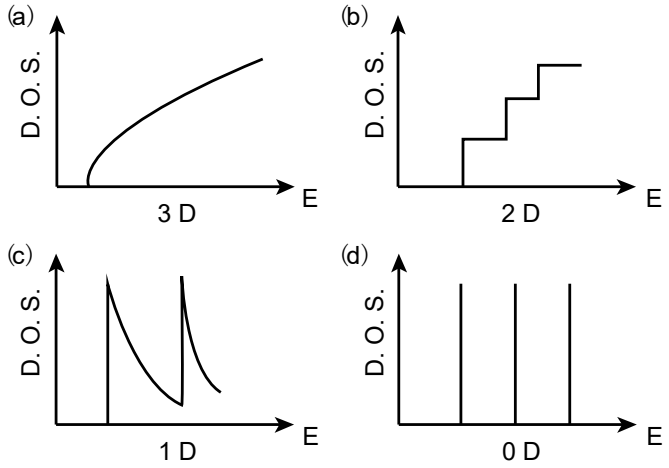

Figure 13 Electronic density of states for (a) a bulk 3D crystalline semiconductor, (b) a 2D quantum well, (c) a 1D nanowire or nanotube, and (d) a 0D quantum dot[130].

Table 3 Seebeck effect of sensing concrete with different functional fillers

Filler		Filler content	Seebeck coefficient (μV/℃)	Absolute thermoelectric power (μV/℃)	References
Carbon material	CF	1.5 vol.%	-3.10	-0.76	Wen et al.[122]
	Expanded graphite	5.0 wt.%	−54.5	-	Wei et al.[125]
	Expanded graphite + CF	5.0 wt.% + 1.2 wt.%	11.59	-	Wei et al.[131]
	n-CNT	1.0 wt.%	-58	-	Tzounis et al.[132]
	p-CNT	1.0 wt.%	20	-	Tzounis et al.[132]
	CNT + CF	0.5 wt.% + 0.4 wt.%	21.7	23.5	Zuo et al.[129]
Metal material	SF	0.2 vol.%	66.2	68.5	Wen et al.[54]
	SS	-	48	-	Tang et al.[133]
	Bi_2Te_3	0.5 wt.%	33.2	35.5	Yao et al.[134]
Metal oxide	Bi_2O_3	5.0 vol.%	97.94	100.28	Wei et al.[135]
	Fe_2O_3	5.0 vol.%	90.23	92.57	Wei et al.[135]
	Nano- Fe_2O_3	5.0 wt.%	2500	-	Ji et al.[130]
	Nano-ZnO	5.0 wt.%	3300	-	Ji et al.[130]
	Nano-MnO_2	5.0 wt.%	-3085	-	Ji et al.[136]

It should be noted that the Seebeck coefficient of sensing concrete also depends on functional filler content. Generally, at any filler content, negative electrons and positive holes contributed additively to the electrical

conductivity, but subtractively to the Seebeck coefficient[137]. In the case of p-type functional fillers such as CF[162] and CNT[89], the increase of filler content before the formation of conductive network is beneficial to transport process of the positive holes in cement paste. If the conductive network is formed, the positive holes tend to diffuse through randomly distributed fillers. Therefore, the quantity of holes that reach the cold end decreases leading to a decrease in Seebeck coefficient[123,138]. While in the case of n-type functional fillers such as MnO_2 and Fe_2O_3, the Seebeck coefficient increases steadily with the increasing filler content as this kind of functional filler is often a semiconductor with a low electrical conductivity compared to conducting fillers such as CF and CNT. However, the high content of functional filler would decrease the flowability of sensing concrete during the fabrication, leading to poor linearity and repeatability of Seebeck effect[136].

The temperature dependence of Seebeck coefficient of sensing concrete has also been reported. Wei et al. found that higher temperature caused lower Seebeck coefficient of sensing concrete with expanded graphite and CFs[131]. In another investigation, they found that with the temperature increased, the Seebeck coefficient of sensing concrete with expanded graphite decreased firstly from 30℃ to 70℃ and then increased from 70℃ to 100℃[125]. The temperature dependence of Seebeck coefficient is attributed to the dependence of electron-hole pairs excited across the energy gap on temperature[125]. However, the use of the Seebeck effect to realize temperature sensing would require the Seebeck coefficient to be stable over a certain temperature range. Therefore, sensing concrete with low temperature-dependence of Seebeck coefficient is still needed to be further investigated. Apart from temperature, the effect of moisture on the Seebeck effect is also very significant. Wei al reported on the Seebeck effect of sensing concrete with expanded graphite and CFs, and performed on purpose measurements at various moisture contents. They found that the increase of moisture content can enhance the Seebeck coefficient[131], which is in good agreement with the finding for sensing concrete with CNTs[132]. With the presence of water, Seebeck effect involves mainly mobility and scattering of either hole or electron charge carriers from functional fillers and movement of ions due to remaining water. On one hand, the water molecules adsorbed on the filler surfaces act as electron donors and endow an n-type thermoelectric behavior governed by electron charge transport[132]. On the other hand, the solid-liquid interfaces among water and other components increase the content of interfaces in a cement matrix. From the microscopic viewpoint of carrier transport, these interface defects would constitute an energy barrier in the direction of the movement of the carrier, thus enhancing the Seebeck effect under the action of scattering and energy filtering effect. Therefore, the Seebeck

coefficient has an increasing tendency as moisture content increases[131].

Besides, attaining a large Seebeck coefficient is not simply a matter of increasing carriers' concentration or mobility. A low thermal conductivity can decrease the flow distance of the carrier because it enables a steep temperature gradient to occur. To evaluate the performance of thermoelectric materials comprehensively, a dimensionless figure of merit (*ZT*) composed of Seebeck coefficient, electrical conductivity, thermal conductivity and absolute measuring temperature is drawn since it determines the conversion efficiency, which is defined as:

$$ZT = \left(\frac{S^2 \delta}{K_E + K_P} \right) T \tag{15}$$

where K_E and K_P are electronic thermal conductivity and phonon thermal conductivity, respectively. $ZT \geq 1$ means the material is suitable for practical applications. According to Equation 15, an excellent thermoelectric material should have high electrical conductivity to minimize Joule heating, a large Seebeck coefficient for the maximum conversion of heat to electrical power, and a low thermal conductivity to prevent thermal shorting. Although higher electrical conductivity and Seebeck coefficient can be obtained respectively while keeping low thermal conductivity, it is difficult to improve them simultaneously as they are oppositely related to carrier concentration. In order to obtain a higher *ZT*, the Seebeck coefficient must be improved in the case of high conductivity, or conversely[125]. Therefore, more effort should be devoted to enhance the Seebeck coefficient and electrical conductivity, to achieve a higher thermoelectric power factor ($S^2\sigma$), to improve the thermoelectric conversion efficiency of sensing concrete to meet the requirements for practical applications.

5. Applications of sensing concrete

To date, the practical applications of sensing concrete mainly focus on SHM and traffic detection as summarized below.

5.1 Structural Health Monitoring

Sensing concrete used for SHM can easily monitor the abnormal change of stress/strain in the damaged parts of structures for ensuring the normal operation of structures. Usually, it can be used in bulk, coating, sandwich, bonded and embedded forms. When the components such as beam, column, plate, ring and brick are wholly made of sensing concrete, this is called bulk form. The application of bulk form has relative simpler construction technology compared to the other four forms[139,140]. The coating form refers to that one surface of a component is covered with a layer of

sensing concrete, and the sandwich form means that the top and bottom surfaces of a component are both covered with sensing concrete layers. In addition, sensing concrete can be prefabricated into sensors with size as conventional coarse aggregate[79]. Then, the small sensors can be attached to concrete component using glue, and this is called bonded form. The embedded form means that the prefabricated sensors are embedded into concrete components to monitor the stress/strain change of damaged parts. Compared with bulk form, the application of coating, sandwich, bonded and embedded forms can greatly improve monitoring efficiency and lower construction cost. Moreover, these four application forms can eliminate the negative impact caused by the high conductivity of sensing concrete, including the threats to human safety and the corrosion of embedded steel[141]. Table 4 shows the main previous research on the application of sensing concrete for SHM in different forms.

Table 4 Previous research on sensing concrete for SHM

Application form	Sensing concrete type	Component	Loading mode	Parameters to monitor	References
Bulk	With CF	Sensing concrete beam	Four-point bending	Elastic compressive stress in the pure bending region	Zhang et al.[142]
				Elastic compressive strain in the pure bending region	
		Sensing concrete beam	Three-point bending	Initial load	Zhang et al.[142]
				Elastic deformation	
				Deflection	
				Fracture	
	With CNF	Sensing concrete column	Compression	Strain	Howser et al.[140]
		Sensing concrete beam	Three-point bending	Strain	Yang et al.[143]
			Four-point bending	Fatigue cumulative damage	
	With CNF/CF/SF	Sensing concrete column	Compression	Damage	Erdem et al.[144]
	With CNT	Sensing concrete beam	Three-point bending	Flexural stress	Adresi et al.[145]
		Sensing concrete beam	Four-point bending	Damage	Downey et al.[146]
		Sensing concrete plate	Impact	Electrical impedance tomography	Downey et al.[147]
			Drilled hole		Gupta et al.[100]

	With waste metallic iron powder	Sensing concrete plate	Drilled hole	Electrical impedance tomography	Dayak et al.[148]
	With TiO_2 particles	Sensing concrete brick	Compression	Stress	Downey et al.[149]
				Strain	
				Crack	
Coating	With CF	Sensing concrete casted on the top or bottom of concrete beam	Three-point bending	Compressive strain of beam surface	Wen et al.[69]
				Tensile strain of beam surface	
		Sensing concrete casted on the bottom of concrete beam	Four-point bending	Damage condition	Howser et al.[140]
				Extent of fatigue damage	
	With CF or CNF	Sensing concrete casted on the top or bottom of reinforced concrete beam	Four-point bending	Strain	Baeza et al.[150]
	With SF	Sensing concrete casted on the top or bottom of reinforced concrete beam	Four-point bending	Damage	Hong et al.[151]
Sandwich	With CF	Sensing concrete on top and bottom of concrete beam	Three-point bending	Stress of compressive and tensile zones within elastic stage	Zheng et al.[152]
				Strain of compressive and tensile zones within elastic stage	
		Sensing concrete on top and bottom of reinforced concrete beam	Four-point bending	Load	Wu et al.[153]
				Deflection	
				Crack	
				Damage extent	
		Sensing concrete on top and bottom of concrete beam	Three-point bending	Loading process	Wen et al.[154]
				Deflection	
	With SF	Sensing concrete on top and bottom of concrete beam	Four-point bending	Loading of compressive and tensile region	Hong et al.[151]
				Deflection of compressive and tensile region	
				Strain of compressive and tensile region	
Bonded	With CF or CNF	Sensing concrete on top, bottom or side of reinforced concrete	Four-point bending	Strain	Baeza et al.[150]

		beam			
	With CNT	Sensing concrete attached on top surface at mid -and quarter-span of reinforced concrete beam	Vibration test	Natural frequency	Ubertini et al.[155]
Embedded	With CF	Concrete cylinder embedded with sensing concrete along its longitudinal axis	Compression	Strain	Chacko et al.[51]
				Crack	
		Sensing concrete embedded into the bottom of concrete beam	Four-point bending	Strain	
				Crack	
	With CF or CNF	Sensing concrete embedded into reinforced concrete beam	Four-point bending	Strain	Baeza et al.[150]
	With CB	Sensing concrete embedded into the center of concrete column	Compression	Strain	Xiao[86]
		Sensing concrete embedded into uniaxial compression, combined compression and shear, and uniaxial tension zones of reinforced concrete beam	Four-point bending	Strain	Xiao[86]
	With CNT	Sensing concrete embedded into tensile region of reinforced concrete beam	Three-point bending	Crack propagation	Vossoughi et al.[156]
				Damage accumulation	
	With hybrid CF and CB	Sensing concrete embedded into compressive zone of reinforced concrete beam	Four-point bending	Stress	Ibarra et al.[157]
				Strain	
		Sensing concrete embedded into its center of concrete column	Uniaxial compression	Stress	
				Strain	
	With hybrid CF and GP	Sensing concrete embedded into its center of concrete column	Compression	Force	Fan et al.[158]
	With self-assembled CNT/NCB	Sensing concrete embedded into its center of concrete column	Compression	Stress	Ding et al.[159]
				Strain	

5.2 Traffic Detection

Traffic parameters, such as traffic flow rates, vehicular speed, vehicle classification and traffic density, are increasingly important for traffic management and pavement design. The detection of these parameters can be achieved by integrating sensing concrete into pavements or bridge sections[82]. The previous researches on sensing concrete for traffic detection are listed in Table 5. The pre-cast or cast-in-place sensing concrete sensors are integrated into pavement mainly in the form of strip component. The detection accuracy of this integrated system is not influenced by polarization and environmental factors, because the change of sensing signal caused by polarization and environmental factors can be filtered out in the post-processing of measured signals. Therefore, the integrated sensing concrete detection system has the advantages of high detection precision, high anti-jamming ability, easy installation and maintenance, long service life, and good structural properties.

Table 5 Previous research on sensing concrete for traffic detection

Sensing concrete type	Application form	Measurement	Parameters to monitor	References
With CF	Sensing concrete roller	Rotate a car tire on the roller in lab	Traffic monitoring Weighing in motion	Shi et al.[160]
	Sensing concrete strip component integrated into pavement	Test sensing concrete response by using testing machine in lab	Vehicle speed detection	Wei [161]
	Sensing concrete strip component integrated into pavement	Test sensing concrete response by using testing machine in lab	Weighting in motion	Jian[162]
With hybrid CF and CB	Sensing concrete strip component integrated into pavement	Test sensing concrete response by using testing machine in lab	Vehicle speed Vehicle weight Traffic flow detection Vehicle type judgment	Gong[163]
With CNT	Sensing concrete strip component integrated into a pavement test section at the Minnesota Road Research Facility	Perform road test at a road research facility with a five-axle semi-trailer truck and a van	Traffic flow monitoring	Han et al.[164]
With NP	Sensing concrete arrays integrated into a pavement	Perform road test at outdoor lab with a car	Passing vehicle detection	Han et al.[165]

6. Conclusions and outlook

This tutorial provides a brief overview on the development and progress of sensing concrete, putting emphasis on the definition, classification, electrically conductive mechanisms, sensing mechanisms, sensing properties including pressure-sensitive property, humidity-sensitive property, temperature-sensitive property and Seebeck effect, and applications of sensing concrete. Apart from the contents discussed in this tutorial, efforts on the hydration process, rheological behavior, mechanical properties, thermal properties, transport properties and electromagnetic properties, etc. of sensing concrete are also numerous and never-ending. Figure 14 summarizes the overall research framework of sensing concrete. Involving from structural material to multifunctional material, sensing concrete is bringing new vigor and vitality into the field of construction materials. Due to the coexistence of structural and sensing functions, sensing concrete has also emerged as an important research topic in the field of SHM. Through the retrospective discussion highlighted above, it can be concluded that the key for the fabrication of sensing concrete is to make it conductive by rationally selecting matrix materials, functional fillers and dispersion agents, and controlling their mix proportions. Nevertheless, there are still plenty of challenges for the practical fabrication of sensing concrete including: 1) desired distribution of functional fillers into matrix materials; 2) strong adhesion between functional filler and matrix materials; 3) complete elimination of dispersion agents on the hydration process and sensing performance; 4) function maximization of functional fillers while at a low concentration; 5) rational adoption of newly developed functional fillers; 6) development of theoretical simulation models able to accurately predict sensing concrete performance; 7) scalable fabrication with high yield and consistency. In addition, due to the essentially same sensing mechanism of various sensing properties, it is inevitable to generate complicated coupling effect among different sensing properties, bringing major challenge in the case of measuring a certain parameter. Therefore, efforts are needed to eliminate the interaction of each sensing property and to facilitate the development and optimization of sensing concrete with tunable sensing property. To explore novel measurement method with compensation circuit associated with decoupling algorithm may be a feasible strategy to overcome this issue. Meanwhile, it is helpful to build multi-component, multi-scale and multi-physics theoretical model for deep understanding of the sensing mechanism and coupling effect of various sensing properties. As the complex service conditions and environments of sensing concrete, study on the long-term evolution of its sensing performance is also an important aspect. With the expanding investigations of nanotechnology, microelectronics, artificial intelligence, 3D printing and digital manufacturing of

concrete, there is a new trend to correlate these advanced techniques with sensing concrete, which will undoubtedly boost the overall properties of sensing concrete. The practical applications of sensing concrete will be also largely extended, not only in the fields of SHM and traffic detection, but also in the applications of military vigilance, environment, energy and communication. In sum, despite various challenges, sensing concrete can make infrastructures smart, eco-efficient, durable and sustainable, and improve the infrastructure operating safety and efficiency and, therefore, is a promising research area in the field of civil engineering.

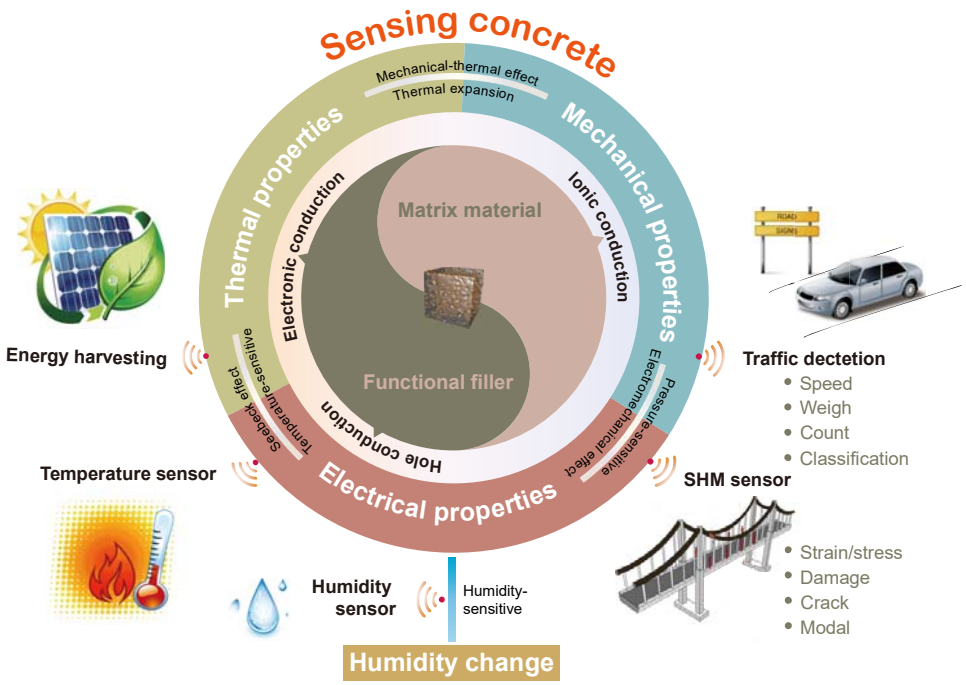

Figure 14 The overall research framework of sensing concrete

Acknowledgements

The authors thank the funding supported from the National Science Foundation of China (51978127 and 51908103), the China Postdoctoral Science Fundation (2019M651116) and the Fundamental Research Funds for the Central Universities in China (DUT18GJ203).

References

1 E. Allen and J. Iano, Fundamentals of Building Construction: Materials and Methods (John Wiley & Sons, 2013).
2 P.D. P. Kumar Mehta and P.D. Paulo J. M. Monteiro, Concrete: Microstructure, Properties, and Materials, Fourth Edition, 4th ed. (McGraw-Hill Education, New York, 2014).
3 B. Han, S. Ding, and X. Yu, Measurement. 59, 110 (2015).
4 J.M. Ko and Y.Q. Ni, Eng. Struct. 27, 1715 (2005).
5 C. Chang, A. Flatau, and S. Liu, Struct. Heal. Monit. 2(3), 257 (2003).

6 S. Das and P. Saha, Measurement. 129, 68 (2018).
7 E.P. Carden and P. Fanning, Struct. Heal. Monit. 3, 355 (2004).
8 S.W. Doebling, C.R. Farrar, and M.B. Prime, Shock Vib. Dig. 30, 91 (1998).
9 W. Hong, J. Zhang, G. Wu, and Z. Wu, Mech. Syst. Signal Process. 50-51, 563 (2015).
10 Y.Y. Li, Mech. Syst. Signal Process. 24, 653 (2010).
11 D. Feng and M.Q. Feng, Mech. Syst. Signal Process. 88, 199 (2017).
12 M. Majumder, T.K. Gangopadhyay, A.K. Chakraborty, K. Dasgupta, and D.K. Bhattacharya, Sensors Actuators A Phys. 147, 150 (2008).
13 S. Taheri, Constr. Build. Mater. 204, 492 (2019).
14 B. Han, Y. Wang, S. Dong, L. Zhang, S. Ding, X. Yu, and J. Ou, J. Intell. Mater. Syst. Struct. 26, 1303 (2015).
15 J.M. López-Higuera, L.R. Cobo, A.Q. Incera, and A. Cobo, J. Light. Technol. 29, 587 (2011).
16 P.W. Chen and D.D.L. Chung, Smart Mater. Struct. 2, 22 (1993).
17 L. Zhang, Nano-Modification Mechanisms and Electrostatic Self-Assembly Nano-Filler Modification of Cement-Based Materials, Dalian University of Technology, 2018.
18 S. Sun, S. Ding, B. Han, S. Dong, X. Yu, D. Zhou, and J. Ou, Compos. Part B Eng. 129, 221 (2017).
19 B. Han, B. Han, and X. Yu, Smart Mater. Struct. 19, 065012 (2010).
20 B. Han, X. Yu, and J. Ou, Self-Sensing Concrete in Smart Structures (Elsevier, 2014).
21 B. Benmokrane, E. El-Salakawy, S. El-Gamal, and S. Goulet, J. Bridg. Eng. 12, 632 (2007).
22 H. Wang, P. Xiang, and L. Jiang, Sensors Actuators A Phys. 285, 414 (2019).
23 H. Zhang, S. Hou, and J. Ou, J. Intell. Mater. Syst. Struct. 27, 418 (2016).
24 S. Muralidharan, V. Saraswathy, K. Thangavel, and N. Palaniswamy, Sensors Actuators B Chem. 130, 864 (2008).
25 G. Song, Y.L. Mo, K. Otero, and H. Gu, Smart Mater. Struct. 15, 309 (2006).
26 C. Yang, Z. Wu, and Y. Zhang, Smart Mater. Struct. 17, (2008).
27 B. Zou, S. Chen, A.H. Korayem, F. Collins, C. Wang, and W. Duan, Carbon. 85, 212 (2015).
28 L. Zhang, S. Ding, B. Han, X. Yu, and Y.Q. Ni, Compos. Part A Appl. Sci. Manuf. 119, 8 (2019).
29 T.C. Hou, V.K. Nguyen, Y.M. Su, Y.R. Chen, and P.J. Chen, Constr. Build. Mater. 133, 397 (2017).
30 A. D'Alessandro, M. Rallini, F. Ubertini, A.L. Materazzi, and J.M. Kenny, Cem. Concr. Compos. 65, 200 (2016).
31 X. Cheng, S. Wang, L. Lu, and S. Huang, J. Compos. Mater. 45, 2033 (2011).
32 M. Saafi, K. Andrew, P.L. Tang, D. McGhon, S. Taylor, M. Rahman, S. Yang, and X. Zhou, Constr. Build. Mater. 49, 46 (2013).
33 X. Liu and S. Wu, Constr. Build. Mater. 25, 1807 (2011).
34 B. Han, S. Sun, S. Ding, L. Zhang, X. Yu, and J. Ou, Compos. Part A Appl. Sci. Manuf. 70, 69 (2015).
35 E. Shamsaei, F.B. de Souza, X. Yao, E. Benhelal, A. Akbari, and W. Duan, Constr. Build. Mater. 183, 642 (2018).
36 M.J. Hanus and A.T. Harris, Prog. Mater. Sci. 58, 1056 (2013).
37 V. Georgakilas, J.A. Perman, J. Tucek, and R. Zboril, Chem. Rev. 115, 4744 (2015).
38 O.A. Mendoza Reales and R. Dias Toledo Filho, Constr. Build. Mater. 154, 697 (2017).
39 B. Han, S. Ding, J. Wang, and J. Ou, Nano-Engineered Cementitious Composites (Springer, Singapore, 2019).
40 H.W. Whittington, J. McCarter, and M.C. Forde, Mag. Concr. Res. 33, 48 (1981).
41 D.D.L. Chung, J. Mater. Eng. Perform. 11, 194 (2002).
42 A.P. Singh, B.K. Gupta, M. Mishra, Govind, A. Chandra, R.B. Mathur, and S.K. Dhawan, Carbon. 56, 86 (2013).
43 V.H. Guerrero, S. Wang, S. Wen, and D.D.L. Chung, J. Mater. Sci. 37, 4127 (2002).
44 S. Stankovich, D.A. Dikin, G.H.B. Dommett, K.M. Kohlhaas, E.J. Zimney, E.A. Stach, R.D. Piner, S.T. Nguyen, and R.S. Ruoff, Nature 442, 282 (2006).
45 I. Balberg, Phys. Rev. Lett. 59, 1305 (1987).
46 Y. Zare, Compos. Part A Appl. Sci. Manuf. 84, 158 (2016).
47 M. Sun, R.J.Y. Liew, M. Zhang, and W. Li, Constr. Build. Mater. 65, 630 (2014).
48 J.G. Simmons, J. Appl. Phys. 34, 1793 (1963).
49 G. Li, P. Wang, and X. Zhao, Cem. Concr. Compos. 29, 377 (2007).
50 Y. Wuang and X. Zhang, Acta Mater. Compos. Sin. 22, 40 (2005).
51 R.M. Chacko, N. Banthia, and A.A. Mufti, Can. J. Civ. Eng. 34, 284 (2007).
52 Z. Wang, Z. Wang, M. Ning, S. Tang, and Y. He, Ceram. Int. 43, 8685 (2017).
53 J.T. Shen, S.T. Buschhorn, J.T.M. De Hosson, K. Schulte, and B. Fiedler, Compos. Sci. Technol. 115, 1 (2015).
54 S. Wen and D.D.L. Chung, Cem. Concr. Res. 30, 661 (2000).
55 M. Sun, Z. Li, Q. Liu, Z. Tang, and D. Shen, Cem. Concr. Res. 30, 1251 (2000).

56 A. Schiessl, W. J. Weiss, J. D. Shane, N. S. Berke, T. O. Mason, and S. P. Shah, Concr. Sci. Eng. 2, 106 (2000).
57 J. Cao and D.D.L. Chung, Cem. Concr. Res. 35, 810 (2005).
58 H.K. Kim, Constr. Build. Mater. 96, 29 (2015).
59 A.T. Hasan and S. Taha, World Appl. Sci. J. 19, 957 (2012).
60 H. Yang, H. Cui, W. Tang, Z. Li, N. Han, and F. Xing, Compos. Part A Appl. Sci. Manuf. 102, 273 (2017).
61 B. Han, X. Guan, and J. Ou, Sensors Actuators, A Phys. 135, 360 (2007).
62 W. Wang, H. Dai, and S. Wu, Mater. Sci. Eng. A (2008).
63 X. Fu and D.D.L. Chung, Cem. Concr. Res. 26, 15 (1996).
64 B. Wu, X. Huang, and J. Lu, Cem. Concr. Res. (2005).
65 B. Han, X. Yu, E. Kwon, and J. Ou, Sens. Lett. 8, 344 (2010).
66 D.G. Meehan, S. Wang, and D.D.L. Chung, J. Intell. Mater. Syst. Struct. 21, 83 (2010).
67 V. Lin, M. Li, J. Lynch and V. Li, in Nondestructive Characterization for Composite Materials, Aerospace Engineering, Civil Infrastructure, and Homeland Security, 798316 (2011).
68 F. Reza, J.A. Yamamuro, and G.B. Batson, Cem. Concr. Compos. (2004).
69 S. Wen and D.D.L. Chung, Cem. Concr. Res. 31, 665 (2001).
70 B. Chen and J. Liu, Constr. Build. Mater. 22, 2196 (2008).
71 S. Wen and D.D.L. Chung, Carbon 44, 1496 (2006).
72 Y. Ding, G. Liu, A. Hussain, F. Pacheco-Torgal, and Y. Zhang, Constr. Build. Mater. 207, 630 (2019).
73 A.L. Materazzi, F. Ubertini, and A. D'Alessandro, Cem. Concr. Compos. 37, 2 (2013).
74 S. Sun, B. Han, S. Jiang, X. Yu, Y. Wang, H. Li, and J. Ou, Constr. Build. Mater. 136, 314 (2017).
75 F. Azhari and N. Banthia, Cem. Concr. Compos. 34, 866 (2012).
76 L. Zhang, S. Ding, L. Li, S. Dong, D. Wang, X. Yu, and B. Han, Compos. Part A Appl. Sci. Manuf. 109, 303 (2018).
77 B. Han, L. Zhang, S. Zeng, S. Dong, X. Yu, R. Yang, and J. Ou, Compos. Part A Appl. Sci. Manuf. 95, 100 (2017).
78 S. Wen and D.D.L. Chung, Carbon N. Y. 45, 263 (2007).
79 B. Han and J. Ou, Sensors Actuators, A Phys. (2007).
80 Y. Ding, Z. Han, Y. Zhang, and J.B. Aguiar, Compos. Struct. (2016).
81 B. Han, L. Zhang, S. Sun, X. Yu, X. Dong, T. Wu, and J. Ou, Compos. Part A Appl. Sci. Manuf. 79, 103 (2015).
82 B. Han, X. Yu, and E. Kwon, Nanotechnology 20, 445501 (2009).
83 B. Han, B. Han, and J. Ou, Sensors Actuators, A Phys. 149, 51 (2009).
84 D.D.L. Chung, Mater. Sci. Eng. R Reports 22, 57 (1998).
85 D. Bloor, A. Graham, E.J. Williams, P.J. Laughlin, and D. Lussey, Appl. Phys. Lett. 88, 86 (2006).
86 H. Xiao, Piezoresistivity of Cement-Based Composite Filled with Nanophase Materials and Self-Sensing Smart Structural System, Harbin Institute of Technology, 2006.
87 E. Teomete, Smart Mater. Struct. 25, (2016).
88 S. Dong, B. Han, J. Ou, Z. Li, L. Han, and X. Yu, Cem. Concr. Compos. 72, 48 (2016).
89 B. Han, Y. Wang, S. Ding, X. Yu, L. Zhang, Z. Li, and J. Ou, J. Intell. Mater. Syst. Struct. 28, 699 (2017).
90 X. Yu and E. Kwon, Smart Mater. Struct. 18, 1 (2009).
91 B. Han, K. Zhang, X. Yu, E. Kwon, and J. Ou, J. Mater. Civ. Eng. 24, 658 (2012).
92 P.C. Ma, N.A. Siddiqui, G. Marom, and J.K. Kim, Compos. Part A Appl. Sci. Manuf. 41, 1345 (2010).
93 F. Sanchez and C. Ince, Compos. Sci. Technol. 69, 1310 (2009).
94 S.H Park, J. Hwang, G.S. Park, J.H. Ha, M. Zhang, D. Kim, D.J. Yun, S. Lee, and S.H. Lee, Nat. Commun. 10, 2537 (2019).
95 S.A.A. El-Enein, M.F. Kotkata, G.B. Hanna, M. Saad, and M.M.A. El Razek, Cem. Concr. Res. (1995).
96 H.K. Kim, I.W. Nam, and H.K. Lee, Compos. Struct. 107, 60 (2014).
97 W.J. McCarter, G. Starrs, and T.M. Chrisp, Cem. Concr. Res. (2000).
98 G.M. Kim, B.J. Yang, K.J. Cho, E.M. Kim, and H.K. Lee, Compos. Struct. (2017).
99 A. Chaipanich, T. Nochaiya, W. Wongkeo, and P. Torkittikul, Mater. Sci. Eng. A (2010).
100 S. Gupta, J.G. Gonzalez, and K.J. Loh, Struct. Heal. Monit. 16, 309 (2017).
101 H.K. Kim, I.S. Park, and H.K. Lee, Compos. Struct. 116, 713 (2014).
102 B. Han, X. Yu, and J. Ou, J. Mater. Sci. 45, 3714 (2010).
103 J. Cao and D.D.L. Chung, Cem. Concr. Res. 34, 481 (2004).
104 B. Han, X. Yu, E. Kwon, and J. Ou, J. Compos. Mater. 46, 19 (2012).
105 W.J. McCarter, J. Am. Ceram. Soc. (1995).

106 T.M. Chrisp, G. Starrs, W.J. McCarter, E. Rouchotas, and J. Blewett, J. Mater. Sci. Lett. 20, 1085 (2001).
107 G.M. Kim, S.M. Park, G.U. Ryu, and H.K. Lee, Cem. Concr. Compos. 82, 165 (2017).
108 L. Zhang, B. Han, J. Ouyang, X. Yu, S. Sun, and J. Ou, Arch. Civ. Mech. Eng. (2017).
109 C. Chang, G. Song, D. Gao, and Y.L. Mo, Smart Mater. Struct. 22, (2013).
110 S. Wen and D.D.L. Chung, Carbon 39, 369 (2001).
111 W.J. McCarter, G. Starrs, T.M. Chrisp, and P.F.G. Banfill, in J. Mater. Sci. (2007).
112 S. Wen, S. Wang, and D.D.L. Chung, Sensors Actuators, A Phys. 78, 180 (1999).
113 E.J. Sellevold and Ø. Bjøntegaard, Mater. Struct. 39, 809 (2006).
114 E. Demircilioğlu, E. Teomete, E. Schlangen, and F.J. Baeza, Constr. Build. Mater. 224, 420 (2019).
115 T.L. Yeo, T. Sun, and K.T.V. Grattan, Sensors Actuators, A Phys. (2008).
116 B. Chen, K. Wu, and W.W. Yao, Cem. Concr. Compos. 26, 291 (2004).
117 G.B.B. Farhad Reza Jerry A. Yamamuro, and Jong S. Lee, ACI Mater. J. 98, (2001).
118 F. Rajabipour and J. Weiss, Mater. Struct. Constr. (2007).
119 B. Han and J. Ou, New Carbon Mater. (2009).
120 B. Han, Z. Yang, X. Shi, and X. Yu, J. Mater. Eng. Perform. 22, 184 (2013).
121 D. Dimov, I. Amit, O. Gorrie, M.D. Barnes, N.J. Townsend, A.I.S. Neves, F. Withers, S. Russo, and M.F. Craciun, Adv. Funct. Mater. 28, 1705183 (2018).
122 S. Wen and D.D.L. Chung, Cem. Concr. Res. 29, 1989 (1999).
123 M. Sun, Z. Li, Q. Mao, and D. Shen, Cem. Concr. Res. 28, 1707 (1998).
124 S. Wen and D.D.L. Chung, Cem. Concr. Res. 31, 507 (2001).
125 J. Wei, L. Zhao, Q. Zhang, Z. Nie, and L. Hao, Energy Build. (2018).
126 M. Sun, Z. Li, Q. Mao, and D. Shen, Cem. Concr. Res. 28, 549 (1998).
127 S. Wen and D.D.L. Chung, Cem. Concr. Res. 30, 1295 (2000).
128 H.Y. Cao, W. Yao, and J.J. Qin, Adv. Mater. Res. (2010).
129 J. Zuo, W. Yao, and K. Wu, Fullerenes Nanotub. Carbon Nanostructures 23, 383 (2015).
130 T. Ji, X. Zhang, and W. Li, Constr. Build. Mater. (2016).
131 J. Wei, Q. Zhang, L. Zhao, L. Hao, and Z. Nie, Ceram. Int. (2017).
132 L. Tzounis, M. Liebscher, R. Fuge, A. Leonhardt, and V. Mechtcherine, Energy Build. (2019).
133 Z. Tang, C. Tong, J. Qian, and Z. WANG, J. Chongqing Jianzhu Univ. 30, 125 (2008).
134 W. Yao and Q. Xia, Gongneng Cailiao 45, 15134 (2014).
135 J. Wei, L. Hao, G. He, and C. Yang, Ceram. Int. 40, 8261 (2014).
136 T. Ji, X. Zhang, X. Zhang, Y. Zhang, and W. Li, J. Mater. Civ. Eng. 30, 04018224 (2018).
137 S. Wen and D.D.L. Chung, J. Mater. Sci. 39, 4103 (2004).
138 J. Wei, Y. Fan, L. Zhao, F. Xue, L. Hao, and Q. Zhang, Ceram. Int. 44, 5829 (2018).
139 O. Galao, E. Zornoza, F.J. Baeza, A. Bernabeu and P. Garcés, Mater. Constr. 62, 343 (2012).
140 R.N. Howser, H.B. Dhonde, and Y.L. Mo, Smart Mater. Struct. 20, 85031 (2011).
141 P. Garcés, L. Ga Andión, I. De la Varga, G. Catalá, and E. Zornoza, Corros. Sci. 49, 2557 (2007).
142 W. Zhang and Xie, J. Southeast Univ. 34, 647 (2004).
143 N. Yang and Q. Sun, Appl. Sci. 9, (2019).
144 S. Erdem, S. Hanbay, and M.A. Blankson, Constr. Build. Mater. 134, 520 (2017).
145 M. Adresi, A. Hassani, J.M. Tulliani, G. Lacidogna, and P. Antonaci, Adv. Cem. Res. 29, 216 (2017).
146 A. Downey, A. D'Alessandro, M. Baquera, E. García-Macías, D. Rolfes, F. Ubertini, S. Laflamme, and R. Castro-Triguero, Eng. Struct. 148, 924 (2017).
147 A. Downey, A. D'Alessandro, F. Ubertini, and S. Laflamme, Meas. Sci. Technol. 29, 35107 (2018).
148 S. Nayak and S. Das, Mater. Des. 175, 107817 (2019).
149 A. Downey, A. D'Alessandro, S. Laflamme, and F. Ubertini, Smart Mater. Struct. 27, 15009 (2018).
150 F.J. Baeza, O. Galao, E. Zornoza, and P. Garcés, Materials (Basel). 6, 841 (2013).
151 L. Hong, W. Sun, and Y. Huang, China Civ. Eng. J. 41, 7 (2008).
152 L. Zheng, X. Song, and Z. Li, J. Huazhong Univ. Sci. Technol. 32, 30 (2004).
153 S. Wu, H. Dai, and W. Wang, Smart Mater. Struct. 16, 2056 (2007).
154 S. Wen and D.D.L. Chung, Adv. Cem. Res. 15, 119 (2003).
155 F. Ubertini, A.L.A.L. Materazzi, A. D'Alessandro, and S. Laflamme, Eng. Struct. 60, 265 (2014).
156 F. Vossoughi, Univ. Calif. (2004).
157 Y. Saéz de Ibarra, J.J. Gaitero, E. Erkizia, and I. Campillo, Phys. Status Solidi a-Applications Mater. Sci. 203,

1076 (2006).
158 X. Fan, D. Fang, M. Sun, and Z. Li, J. Wuhan Univ. Technol. Sci. Ed. 26, 339 (2011).
159 S. Ding, Y. Ruan, X. Yu, B. Han, and Y.Q. Ni, Constr. Build. Mater. 201, 127 (2019).
160 Z.Q. Shi and D.D.L. Chung, Cem. Concr. Res. 29, 435 (1999).
161 W.B. Wei, A Research of the Traffic Vehicle-Speed Measuring System Based on the Pressure-Sensitivity of CFRC, Shantou University, 2003.
162 H.L. Jian, Research of the Traffic Weighting Monitoring System Based on the Pressure-Sensitivity of CFRC, Shantou University, 2004.
163 Z.Q. Gong, Research of the Traffic Monitoring System Based on the Pressure-Sensitivity of CFRM, Shantou University, 2007.
164 B. Han, K. Zhang, T. Burnham, E. Kwon, and X. Yu, Smart Mater. Struct. 22, 015020 (2013).
165 B. Han, K. Zhang, X. Yu, E. Kwon, and J. Ou, Measurement 44, 1645 (2011).